

TI Designs: TIDA-01067

Smart Damper Control Reference Design With Pressure, Humidity, and Temperature Sensing



Description

The TIDA-01067 design is built to enable multiple room comfort control in connected HVAC systems. Sensing temperature, humidity, and pressure allows independent monitoring and air-flow adjustment in each zone. This TI Design converts a constant air volume (CAV) into a variable air volume (VAV) system. Collected data can be transmitted wirelessly to the smart thermostat or gateway. Onboard sensors can be employed to allow predictive maintenance, shorten technical troubleshooting time, and reduce overall energy consumption. Long battery life allows the smart damper to run for many years without the need to spend time and money on battery replacement.

Resources

TIDA-01067	Design Folder
DRV8833	Product Folder
CC2650	Product Folder
TPS62745	Product Folder
HDC1010	Product Folder
CSD25310Q2	Product Folder
TPD1E10B06	Product Folder



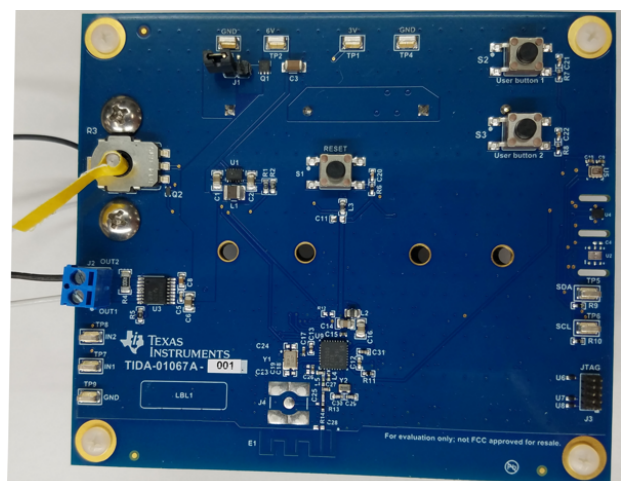
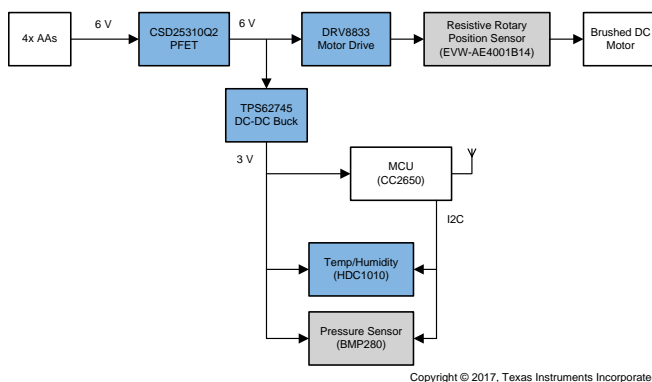
[ASK Our E2E Experts](#)

Features

- SimpleLink™ Software Platform
- Integrated *Bluetooth*® Low Energy Radio and MCU for Smaller Form Factor
- Configurable Advertisement Interval up to 4 Seconds
- Ultra-Low-Power Consumption:
 - Total Average Current of 30.56 μA (Five Louver Adjustment Events per day)
 - 3.7- μA Standby Current
 - 61- $\mu\text{A}/\text{MHz}$ ARM® Cortex®-M3
 - DC-DC Converter Uses 28 μA of Average Power (500-ms Advertisement Intervals)
- Operates on Four AA Batteries
- Motor Driver Has Integrated FETs and Current Sense Comparator, Enabling Easy Design, and Small Solution Size With Minimal Discretes

Applications

- HVAC Valve and Actuator Control
- Electronic Smart Lock
- Motorized Window Blinds
- Wireless Environmental Sensor
- Building Automation
- HVAC Motor Control





An IMPORTANT NOTICE at the end of this TI reference design addresses authorized use, intellectual property matters and other important disclaimers and information.

1 System Description

In the ecosystem of smart thermostats and HVAC systems, the next step is to collect data from the vents within the building to capture a snap shot of environmental conditions in the home or building. With several smart damper controllers in the vent system at critical, un-monitored ventilation points in the building, temperature can be controlled more efficiently using algorithms to create a balanced temperature and pressure throughout. Onboard sensors can allow real-time diagnostics, analysis of historical trends, predictive maintenance, shorten technical troubleshooting time, and reduce overall energy consumption. Replacing multiple batteries can be a timely and costly issue, therefore lowering the average current consumption is often a key design consideration.

Enabled by TI's light load efficient DC-DC converter, SimpleLink ultra-low-power wireless MCU platform, integrated motor driver, this design guide demonstrates how a light load efficient power topology can increase battery life based on low standby current and long off-state intervals. This design guide addresses component selection, design theory, and test results of the TI Design system. The scope of this design guide gives system designers a head-start in implementing a low-power smart damper control design for HVAC dampers, smart locks, wireless automatic blinds, and actuators.

1.1 Key System Specifications

Table 1. Key System Specifications

PARAMETER	SPECIFICATION	DETAILS
Input power source	Four AA alkaline batteries (operating range from 3.7 to 6.4 V)	See Section 4.2.1.1
Bluetooth low energy advertisement interval	500 ms	See Section 4.2.2
Average Bluetooth low energy and MCU current consumption	26- μ A average (24-hour period)	See Section 4.2.2
Average losses of power topologies (by design)	LDO: 366.9 μ W	See Section 2.3.9
	Buck: 30.7 μ W	
	Boost: 349.9 μ W	
Louver adjustment events	Five events per day	—
Motor type	Brushed DC	See Section 4.1.3
Motor current	21-mA average (2-A max)	See Section 4.2.4
Environmental sensing event (pressure, temperature, and humidity)	105- μ A average (per event, 120 milliseconds)	See Section 4.2.5
User interface	3 buttons	See Section 3.1
Total system power consumption	30- μ A average	See Section 4.2.6.5
Estimated battery life	10.08 years	See Section 4.2.6.6
Test results	5.0 V, 25°C, five events, 500 ms	See Section 4.2

2 System Overview

2.1 Block Diagram

Figure 1 shows the TIDA-01067 block diagram.

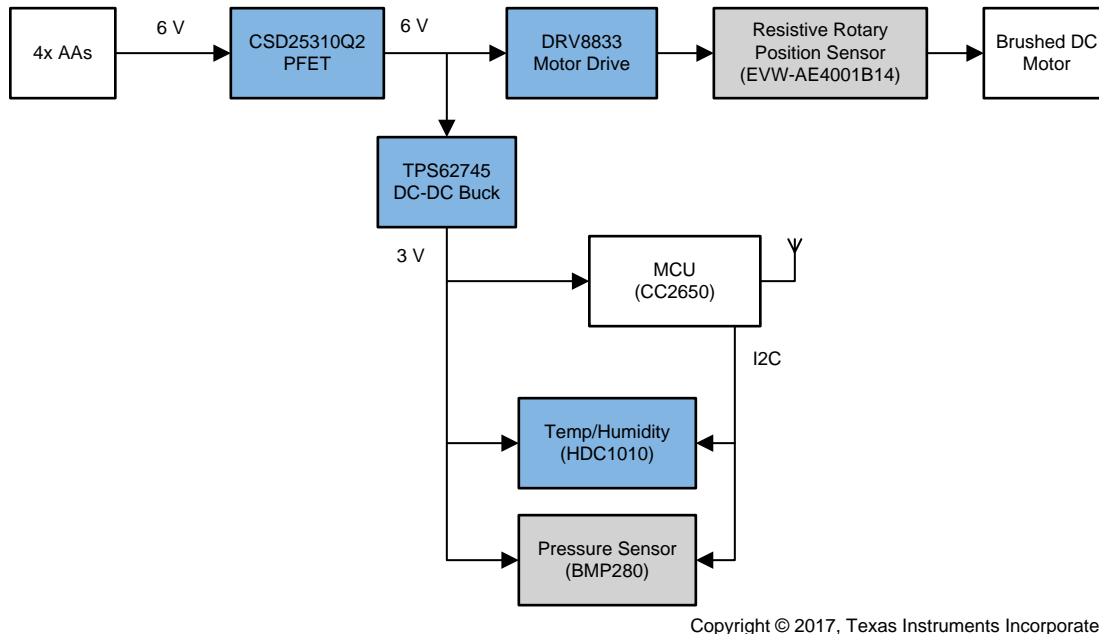


Figure 1. TIDA-01067 Block Diagram

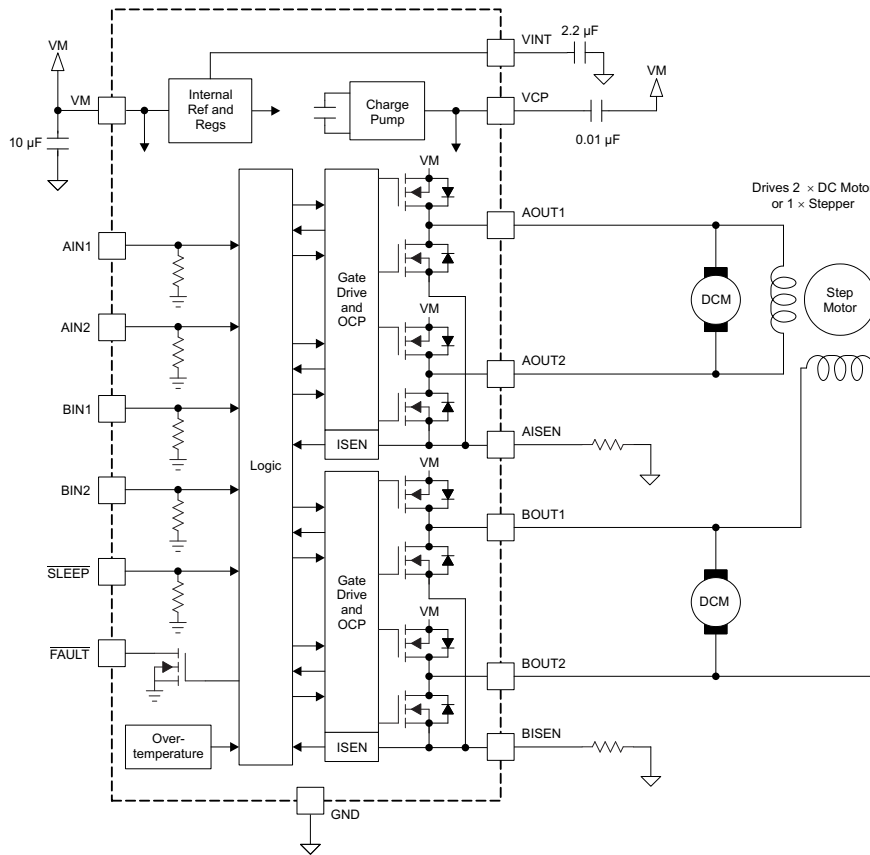
2.2 Highlighted Products

This TI Design features the following devices:

- DRV8833 (Section 2.2.1): Dual H-bridge motor driver with motor current control and low R_{DSon} of 360 m Ω
- CC2650 (Section 2.2.2): 2.4-GHz Bluetooth low energy with a ultra-low-power wireless MCU (32-bit ARM Cortex-M3 processor)
- TPS62745 (Section 2.2.3): Ultra-low I_Q buck converter with 16 selectable output voltages from 1.8 to 3.3 V and 90% efficiency at load currents $\geq 15 \mu A$
- HDC1010 (Section 2.2.4): Digital humidity sensor with integrated temperature sensor
- CSD25310Q2 (Section 2.2.5): Low-cost power PFET with gate-to-source voltage of $\pm 8 V$ and low R_{DSon} of 19 m Ω
- TPD1E10B06 (Section 2.2.6): Single-channel ESD in a 0402 package with 10-pF capacitance and 6-V breakdown

2.2.1 DRV8833

The device has two H-bridge drivers, and can drive two DC brush motors, a bipolar stepper motor, solenoids, or other inductive loads (see Figure 2). The output driver block of each H-bridge consists of N-channel power MOSFETs configured as an H-bridge to drive the motor windings. Each H-bridge includes circuitry to regulate or limit the winding current. Internal shutdown functions with a fault output pin are provided for overcurrent protection, short-circuit protection, undervoltage lockout, and overtemperature. A low-power sleep mode is also provided.



Copyright © 2016, Texas Instruments Incorporated

Figure 2. DRV8833 Block Diagram

DRV8833 features:

- Dual H-bridge current-control motor driver
 - Can drive two DC motors or one stepper motor
 - Low MOSFET ON-resistance: HS + LS 360 mΩ
- Output current (at $V_M = 5\text{ V}$, 25°C)
 - 1.5-A RMS, 2-A peak per H-bridge in PWP and RTY package options
 - 500-mA RMS, 2-A peak per H-bridge in PW package option
- Outputs can be in parallel for:
 - 3-A RMS, 4-A peak (PWP and RTY)
 - 1-A RMS, 4-A peak (PW)
- Wide power supply voltage range: 2.7 to 10.8 V
- PWM winding current regulation and current limiting
- Thermally enhanced surface-mount packages

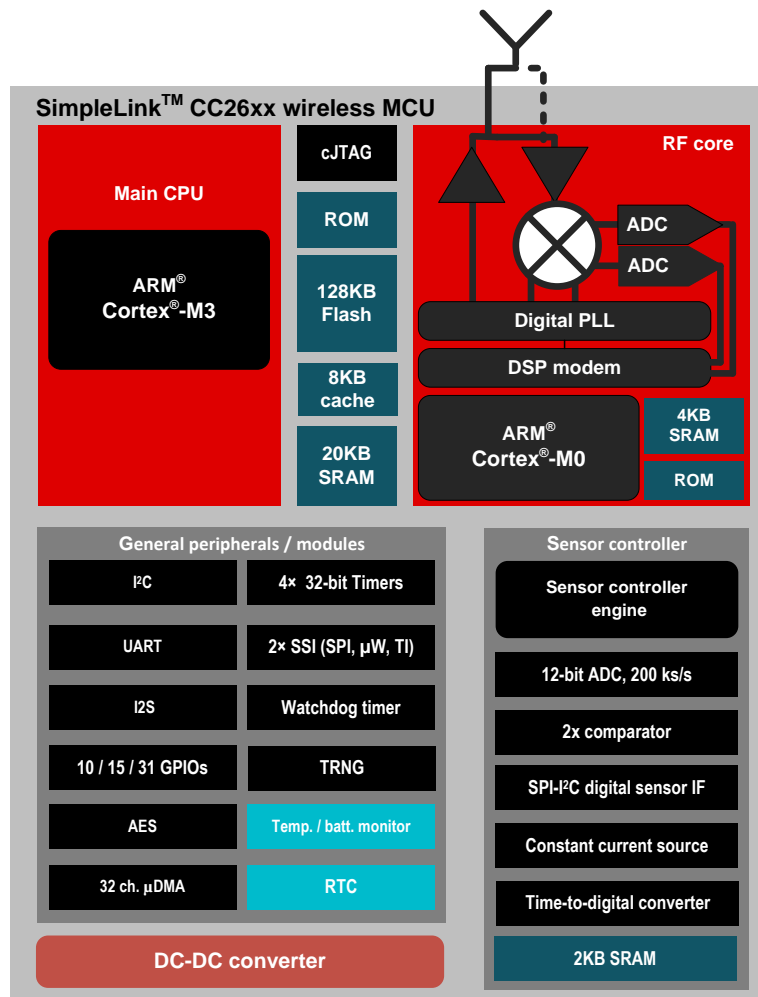
2.2.2 CC2650

The CC2650 device is a wireless MCU targeting Bluetooth, ZigBee® and 6LoWPAN, and ZigBee RF4CE remote control applications.

The device is a member of the CC26xx family of cost-effective, ultra-low-power, 2.4-GHz RF devices. Very low active RF and MCU current and low-power mode current consumption provide excellent battery lifetime and allow for operation on small coin-cell batteries and in energy-harvesting applications.

The CC2650 device contains a 32-bit ARM Cortex-M3 processor that runs at 48 MHz as the main processor and a rich peripheral feature set that includes a unique ultra-low-power sensor controller. This sensor controller is ideal for interfacing external sensors and for collecting analog and digital data autonomously while the rest of the system is in sleep mode. Thus, the CC2650 device is ideal for applications within a whole range of products including industrial, consumer electronics, and medical.

The Bluetooth low energy (BLE) controller and the IEEE 802.15.4 MAC are embedded into ROM and are partly running on a separate ARM Cortex-M0 processor. This architecture improves overall system performance and power consumption and frees up flash memory for the application. The Bluetooth stack is available free of charge from www.TI.com.



Copyright © 2016, Texas Instruments Incorporated

Figure 3. CC2650 Block Diagram

CC2650 features:

- Microcontroller:
 - Powerful ARM Cortex-M3
 - EEMBC CoreMark® score: 142
 - Up to 48-MHz clock speed
 - 128KB of in-system programmable flash
 - 8KB of SRAM for cache
 - 20KB of ultra-low-leakage SRAM
 - Two-pin cJTAG and JTAG debugging
 - Supports over-the-air (OTA) upgrade
- Ultra-low-power sensor controller:
 - Can run autonomous from the rest of the system
 - 16-bit architecture
 - 2KB of ultra-low-leakage SRAM for code and data
- Efficient code size architecture, placing drivers, Bluetooth low energy controller, and bootloader in ROM
- RoHS-compliant packages:
 - 4-mm×4-mm RSM VQFN32 (10 GPIOs)
 - 5-mm×5-mm RHB VQFN32 (15 GPIOs)
 - 7-mm×7-mm RGZ VQFN48 (31 GPIOs)
- Peripherals:
 - All digital peripheral pins can be routed to any gpio
 - Four general-purpose timer modules (eight 16-bit or four 32-bit timers, PWM each)
 - 12-bit ADC, 200-ksamples/s, 8-channel analog MUX
 - Continuous time comparator
 - Ultralow-power analog comparator
 - Programmable current source
 - UART
 - 2× SSI (SPI, MICROWIRE, TI)
 - I²C
 - I²S
 - Real-time clock (RTC)
 - AES-128 security module
 - True random number generator (TRNG)
 - 10, 15, or 31 GPIOs, depending on package option
 - Support for eight capacitive-sensing buttons
 - Integrated temperature sensor
- External system:
 - On-chip internal DC-DC converter
 - Very few external components
 - Seamless integration with the SimpleLink CC2590 and CC2592 range extenders
 - Pin compatible with the SimpleLink CC13xx in 4-mm×4-mm and 5-mm×5-mm VQFN packages
- Low power:
 - Wide supply voltage range:
 - Normal operation: 1.8 to 3.8 V
 - External regulator mode: 1.7 to 1.95 V

- Active-mode RX: 5.9 mA
- Active-mode TX at 0 dBm: 6.1 mA
- Active-mode TX at 5 dBm: 9.1 mA
- Active-mode MCU: 61 μ A/MHz
- Active-mode MCU: 48.5 CoreMark/mA
- Active-mode sensor controller: 8.2 μ A/MHz
- Standby: 1 μ A (RTC running and RAM/CPU retention)
- Shutdown: 100 nA (wake up on external events)
- RF section:
 - 2.4-GHz RF transceiver compatible with Bluetooth low energy 4.2 specification
 - Excellent receiver sensitivity (–97 dBm for Bluetooth low energy), selectivity, and blocking performance
 - Link budget of 102 dB/105 dB (BLE/802.15.4)
 - Programmable output power up to 5 dBm
 - Single-ended or differential RF interface
 - Suitable for systems targeting compliance with worldwide radio frequency regulations:
 - ETSI EN 300 328 (Europe)
 - EN 300 440 Class 2 (Europe)
 - FCC CFR47 Part 15 (US)
 - ARIB STD-T66 (Japan)
- Tools and development environment:
 - Full-feature and low-cost development kits
 - Multiple reference designs for different RF configurations
 - Packet sniffer PC software
 - Sensor controller studio
 - SmartRF™ Studio
 - SmartRF Flash Programmer 2
 - IAR Embedded Workbench® for ARM
 - Code Composer Studio™

2.2.3 TPS62745

The TPS62745 is a high-efficiency ultra-low-power, synchronous step-down converter optimized for low-power wireless applications. The device provides a regulated output voltage consuming only a 400-nA quiescent current. The device operates from two rechargeable Li-Ion batteries, Li-primary battery chemistries such as Li-SOCl₂, Li-SO₂, Li-MnO₂, or four- to six-cell alkaline batteries. The input voltage range is set with four VSEL pins from 1.8 to 3.3 V for TPS62745 or 1.3 V and 2.8 V for the TPS627451. The TPS62745 features low output ripple voltage and low noise with a small output capacitor. An internal input voltage switch controlled by pin EN_VIN_SW connects the supply voltage to pin VIN_SW. The switch is intended to be used for an external voltage divider, scaling down the input voltage for an external ADC. The switch is automatically opened when the supply voltage is below the undervoltage lockout threshold. The TPS62745 is available in a small, 12-pin 3-mm×2-mm WSON package.

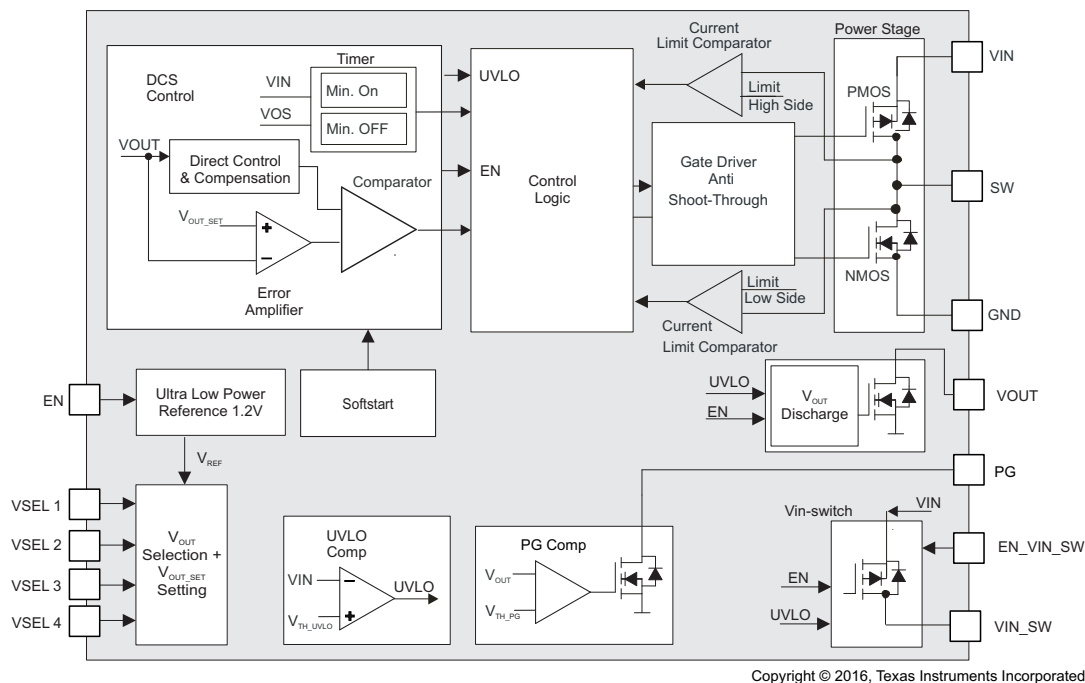


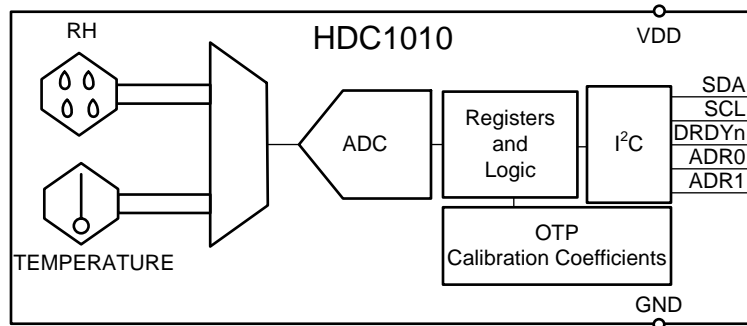
Figure 4. TPS62745 Block Diagram

TPS62745 features:

- Input voltage range V_{IN} from 3.3 to 10 V
- Typical 400-nA quiescent current
- Up to 90% efficiency with load currents > 15 μ A
- Up to 300-mA output current
- RF friendly DCS-Control™
- Low output ripple voltage
- 16 selectable output voltages from:
 - 1.8 to 3.3 V (TPS62745)
 - 1.3 to 2.8 V (TPS627451)
- Integrated input voltage switch
- Integrated discharge function at VOUT
- Open-drain power good output
- Operates with a tiny 3.3- or 4.7- μ H inductor
- Small 3-mm×2-mm WSON package

2.2.4 HDC1010

The HDC1010 is a digital humidity sensor with integrated temperature sensor that provides excellent measurement accuracy at very low power. The sensing element of the HDC1010 is placed on the bottom part of the device, which makes the HDC1010 more robust against dirt, dust, and other environmental contaminants. Measurement results can be read out through the I²C-compatible interface. Resolution is based on the measurement time and can be 8, 11, or 14 bits for humidity, and 11 or 14 bits for temperature.



Copyright © 2016, Texas Instruments Incorporated

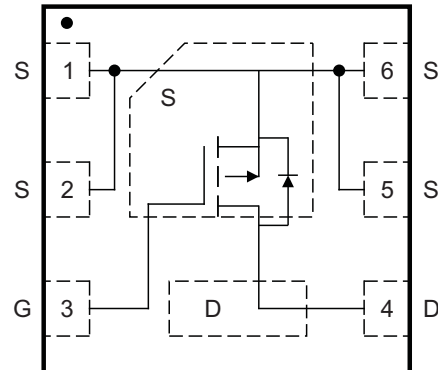
Figure 5. HDC1010 Block Diagram

HDC1010 features:

- Relative humidity accuracy $\pm 2\%$ (typical)
- Temperature accuracy $\pm 0.2^\circ\text{C}$ (typical)
- Excellent stability at high humidity
- 14-bit measurement resolution
- 100-nA sleep mode current
- Average supply current:
 - 710 nA at 1 sps, 11-bit RH measurement
 - 1.3 μA at 1 sps, 11-bit RH and temperature measurement
- Supply voltage: 2.7 to 5.5 V
- Tiny 2-mm \times 1.6-mm device footprint
- I²C interface: Three independent program execution engines, nine programmable outputs with a 25.5-mA full-scale current, 8-bit current-setting resolution, and a 12-bit PWM control resolution

2.2.5 CSD25310Q2

This 19.9-m Ω , -20-V P-channel device is designed to deliver the lowest ON-resistance and gate charge in the smallest outline possible with excellent thermal characteristics in an ultra-low profile. Its low ON-resistance coupled with an extremely small footprint in a SON 2-mm \times 2-mm plastic package make the device ideal for battery-operated, space-constrained operations.



P0112-01

Copyright © 2017, Texas Instruments Incorporated

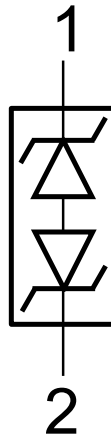
Figure 6. CSD25310Q2 Device Configuration

CSD25310Q2 features:

- Ultra-low Q_g and Q_{gd}
- Low ON resistance
- Low thermal resistance
- Pb-free
- RoHS compliant
- Halogen free
- SON 2-mm \times 2-mm plastic package

2.2.6 TPD1E10B06

The TPD1E10B06 device is a single-channel electrostatic discharge (ESD) transient voltage suppression (TVS) diode in a small 0402 package. This TVS protection product offers ± 30 -kV contact ESD, ± 30 -kV IEC air-gap protection, and has an ESD clamp circuit with a back-to-back TVS diode for bipolar or bidirectional signal support. The 12-pF line capacitance of this ESD protection diode is suitable for a wide range of applications supporting data rates up to 400 Mbps. The 0402 package is an industry standard and is convenient for component placement in space-saving applications.



Copyright © 2016, Texas Instruments Incorporated

Figure 7. TPD1E10B06 Block Diagram

TPD1E10B06 features:

- Provides system-level ESD protection for low-voltage I/O interface
- IEC 61000-4-2 level 4 ESD protection:
 - ± 30 -kV contact discharge
 - ± 30 -kV air-gap discharge
- IEC 61000-4-5 surge: 6 A (8/20 μ s)
- I/O capacitance 12 pF (typical)
- R_{DYN} 0.4 Ω (typical)
- DC breakdown voltage ± 6 V (minimum)
- Ultra-low leakage current 100 nA (maximum)
- 10-V clamping voltage (maximum at $I_{PP} = 1$ A)
- Industrial temperature range: -40°C to 125°C
- Space-saving 0402 footprint (1 mm \times 0.6 mm \times 0.5 mm)

2.3 System Design Theory

This reference design uses the CC2650 MCU with integrated Bluetooth low energy radio device to wirelessly adjust the louver position of an HVAC vent: monitoring the battery voltage for low-life indication, limiting the current through the motor (great for the life of the motor), and communicating these events back to the user. This TI Design achieves an extremely long battery life through the choice of power topology, in this case a highly-efficient buck converter, the TPS62745, and through the use of extending the duty cycle of the Bluetooth low energy connection events.

There are four main devices in this smart damper control design: the MCU, Bluetooth radio, motor driver, and power management. The TIDA-01067 focuses on these four devices (three in this case since the CC2650 is an MCU with integrated Bluetooth radio) and their equations used for average power consumption to determine the life of the batteries. Once the average power per device is calculated, then it is possible to calculate the battery life in milliwatt-hours (mWh). To calculate the battery life, two different current scenarios are examined:

- When the Bluetooth is on and sending out a connection event every 500 ms (or any other value chosen by the user)
- When an adjustment event signals the motor driver to pump around 1 A of current through the DC motor

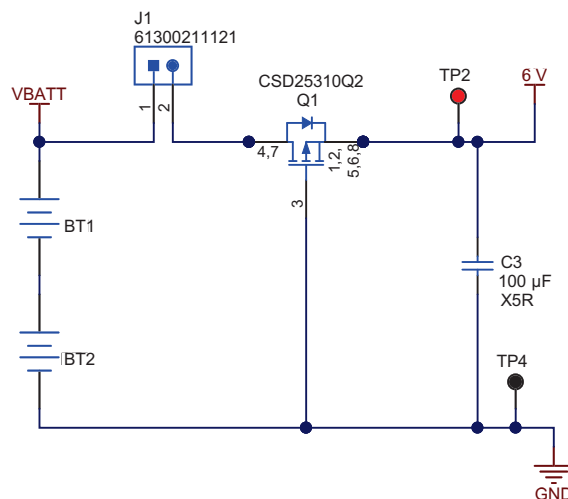
This TI Design ignores the time when the Bluetooth is paired because usually this means an event is about to occur, and the amount of current delivered through the motor is almost two orders of magnitude higher than the current flowing to the Bluetooth device. For the purpose of this design guide, an event is when a user or sensing algorithm has set a new louver position value into the "position" register. For example, if the user decides they want more airflow from a certain vent and adjusts the angle of the louver, that is considered one event. Another event would be when the master system decides that a vent needs to be opened to balance the pressure in the ductwork.

2.3.1 Battery Choice

Batteries were chosen for two main reasons: capacity and popularity of the battery platform. AA batteries have a greater capacity than AAA batteries. Also, at the time of this writing, AA batteries are used in more applications similar to the smart damper in the present-day market.

2.3.2 Reverse Polarity Protection

Figure 8 shows the reverse polarity protection.



Copyright © 2017, Texas Instruments Incorporated

Figure 8. Battery Polarity Protection Schematic

A PFET or an NFET can be used to protect against reverse polarity protection. However, a PFET was used in this TI Design because the PFET does not break up the ground circuit as an equivalent NFET circuit does.

2.3.2.1 Using a FET

The most recent MOSFETs are very low resistance and therefore ideal for providing reverse current protection with minimal loss. [Figure 9](#) shows a low-side NMOS FET in the ground return path, and [Figure 10](#) shows a high-side PMOS FET in the power path.

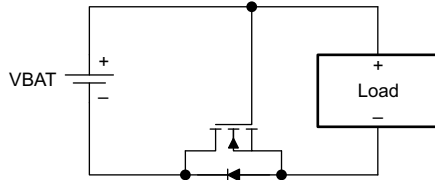


Figure 9. NMOS FET Ground Return Path

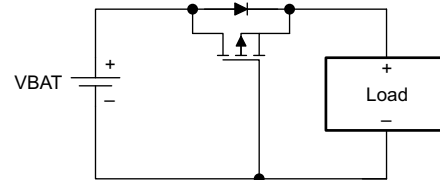


Figure 10. PMOS FET Power Path

In each circuit, the body diode of the FET is oriented in the direction of normal current flow. When the battery is installed incorrectly, the NMOS (PMOS) gate voltage of the FET is low (high), preventing it from turning on. When the battery is installed properly and the portable equipment is powered, the NMOS (PMOS) gate voltage of the FET is taken high (low), and its channel shorts out the diode.

A voltage drop of $R_{DS(on)} \times I_{LOAD}$ is seen in the ground return path when using the NMOS FET, and in the power path when using the PMOS FET. In the past, the primary disadvantage of these circuits has been the high cost of low $R_{DS(on)}$, low-threshold voltage FETs. However, advances in semiconductor processing have resulted in FETs which provide minimal drops in small packages.

2.3.3 Power Topologies

Three main power topologies are possible for this smart damper application: low dropout (LDO) regulator, step-down converter (also known as buck), and boost (see Figure 11). The LDO and buck implementations are not event dependent, meaning the two topologies use the same amount of energy regardless of how many louver adjustment events occur in a day. The LDO and buck drop the voltage down to generate the lower voltage power rail to run the MCU, and the higher voltage components are run off the higher battery voltage. The boost is event dependent because each louver adjustment event must boost up the voltage from 3 to 5 V for motor operation.

A buck configuration was chosen because the LDO has ground leakage current, whereas the buck has zero ground leakage current and therefore more efficiency. More analysis into power topologies is covered in Section 2.3.9.

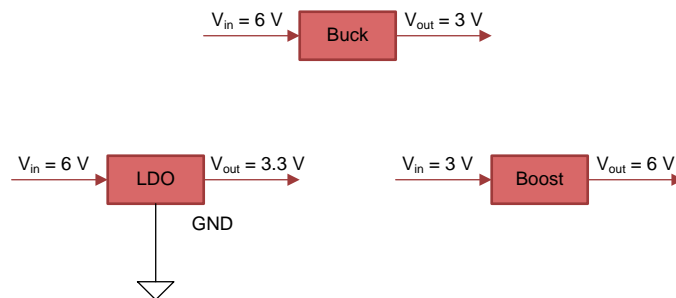


Figure 11. Power Topologies

The TPS62745 step-down converter was chosen because of the extra benefits it offers for low-power designs. This TPS device has select lines that allow the user to select the output voltage, and therefore removes the need for a feedback resistor. The BOM cost can be decreased slightly because there is no feedback resistor. The TPS62745 can dynamically enable or disable the battery voltage check with the use of an enable pin and external resistor voltage divider. Energy is conserved because the voltage divider is only enabled when a battery voltage check is necessary. The rest of the time the divider circuitry does not use energy and is not connected. The TPS62745 is also efficient at extremely light loads; it is 85% efficient at 10 μ A.

2.3.4 MCU With Integrated Bluetooth Low Energy Radio

This reference design must connect and communicate with a central device. However, because power consumption is a concern in battery-based applications, the radio and processor must be low power. Also, the wireless protocol required for the end-equipment system is an important consideration for the selection of the radio device. With TI's SimpleLink ultra-low-power wireless MCU platform, low power with a combined radio and MCU enables extremely long battery life for sensor end nodes. Furthermore, the CC2650 device is a multistandard device, targeting Bluetooth low energy, ZigBee, 6LoWPAN, and ZigBee RF4CE remote control applications. In this TI Design, Bluetooth low energy is the protocol of choice, but the hardware can work with other protocols as well.

2.3.5 Motor Driver

Drive current, power-supply voltage range, load motor types, and safety shutdown functions were all factors when choosing a motor driver. The DRV8833 includes all of the necessary features. The DRV8833 can drive many types of motors and inductive loads, with a peak current of 2 A and a power-supply voltage range of 2.7 to 10.8 V, making it ideal to run off of four AA batteries. The nominal drive voltage is 5 V from the batteries. The major discriminating factor of the DRV8833 is the ability to clamp the current at a certain level determined by the external resistor. The DRV8833 has a current-sense function, which allows the driver to monitor and adjust the output current so the motor does not burned out or waste power from the battery. The motor can be protected by setting the DRV8833 current limit below the motor stall current.

2.3.6 Humidity and Temperature Sensor

An integrated humidity and temperature sensor decreases complexity of system design and overall footprint of the finished product. With one read command, the temperature and humidity can be collected from the HDC1010. The use of a single device saves power and decreases communication time and cycles needed to collect necessary information. The humidity and temperature data is important for HVAC diagnostics and controlling the temperature differences between zones. With the data collection and connected nature of this TI Design, the device can act as a sensor node and transmit the environment data to a gateway or to another device that can communicate this information over the web.

2.3.7 Pressure Sensor

A small footprint, low-power pressure sensor is ideal for this application where battery life and solution size are important features. An I²C interface makes it easy to read, write, and configure the pressure sensor. The Bosch BMP280 sensor fits all of these characteristics. The BMP has very low sleep current (0.1 μ A) and can wake up quickly to take a reading and go back to sleep.

2.3.8 Bluetooth Low Energy and MCU Connection Interval and Average Power Consumption

Because of this system topology, the CC2650 only uses the first current scenario described in [Section 2.3](#). [Figure 12](#) shows a typical current waveform. The period between connection events can be programmed from 10 ms to 4 s in the Bluetooth stack. The pulse-width of the connection event current (or on current) is at 5 ms.

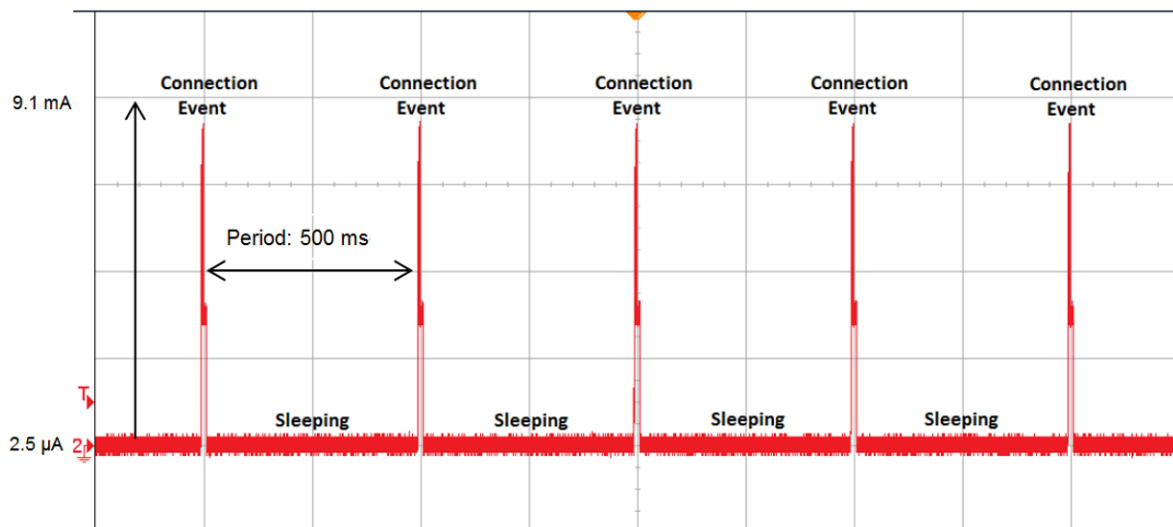


Figure 12. Current Consumption versus Time During Bluetooth Low Energy Connections

The main parameters of the Bluetooth and MCU which affect the total estimated battery life are as follows:

- The supply voltage: $V_{\text{supply}} = 3 \text{ V}$
- The on current: $I_{\text{on}} = 9.1 \text{ mA}$
- The off current: $I_{\text{off}} = 2.5 \text{ } \mu\text{A}$
- The on-duty cycle: $D_{\text{on}} = t_{\text{on}} / T = 5 \text{ ms} / 500 \text{ ms} = 1\%$
- The off-duty cycle: $D_{\text{off}} = 1 - D_{\text{on}} = 99\%$

Equation 1 describes the average power consumed during operation with values taken from their respective datasheets.

$$P_{BLE} = (V_{supply}) \times (I_{on}) \times (D_{on}) + (V_{supply}) \times (I_{off}) \times (D_{off})$$

$$P_{BLE} = (3V) \times (9.1\text{ mA}) \times (0.01) + (3V) \times (2.5\mu\text{A}) \times (0.99) = 280.4\mu\text{W} \quad (1)$$

The current waveform in Figure 12 occurs until the batteries expires, regardless of how many times the user wirelessly adjust the louver position.

2.3.9 Power Topologies: LDO Versus Buck Versus Boost

A smart damper system can use three different types of power topologies: LDO, buck, and boost. These regulators transfer power from the input to the output. Not all of the power is transferred to the output, some of it is lost. The efficiency of each device is measured by how much of the power is transferred to the output from the input. The LDO and buck topology powers the Bluetooth radio, MCU, humidity or temperature sensor and pressure sensor, or an LED driver as in this example, where as the motor driver is powered straight from the four AA batteries. The boost topology does the complete opposite and powers the motor driver while the batteries power up the other devices. The voltage of four AA batteries is 6 V, but it only lasts for a short time as seen on alkaline battery life curves. A typical one-cell AA battery (and AAA) usually has a voltage of 1.25 V for the majority of its life.

The following equations use this 1.25 V-rating per cell—5 V for a four-cell battery—because it is a more accurate measurement for average power loss. Both the LDO and buck topology use the 4s1p battery configuration, while the boost configuration uses the 2s2p configuration. Again, the average power equations used in this section are power losses and not power consumed. This section includes power loss equations of all three topologies to better choose a power topology for a smart damper design.

2.3.9.1 LDO

The main parameters of the LDO regulator that affect the total estimated battery life are:

- The input voltage: $V_{in} = 5\text{ V}$ (four AA batteries in series, nominal voltage)
- The output voltage: $V_{out} = 3\text{ V}$
- The output on current: $I_{on} = 9.1\text{ mA}$
- The output off current: $I_{off} = 5\mu\text{A}$
- The ground current: $I_{gnd} = 35\mu\text{A}$ (this value could be higher depending on the LDO)
- The on-duty cycle: $D_{on} = t_{on} / T = 5\text{ ms} / 500\text{ ms} = 1\%$
- The off-duty cycle: $D_{off} = 1 - D_{on} = 99\%$

Equation 2 describes the average power loss of the LDO during operation.

$$P_{LDO} = (V_{in} - V_{out}) \times (I_{on}) \times (D_{on}) + (V_{in} - V_{out}) \times (I_{off}) \times (D_{off}) + (V_{in}) \times (I_{gnd})$$

$$P_{LDO} = (5V - 3V) \times (9.1\text{ mA}) \times (0.01) + (5V - 3V) \times (5\mu\text{A}) \times (0.99) + (5V) \times (35\mu\text{A}) = 366.9\mu\text{W} \quad (2)$$

The I_{off} current is at $5\mu\text{A}$ because of the quiescent current of both the Bluetooth low energy device (CC2650) and an LED driver (LP55231). The I_{gnd} current value can be taken from any LDO regulator datasheet. On some datasheets, this value can also be referred to as the quiescent current. I_{gnd} is the difference between the input current and the output current, and it is a key characteristic for differentiating the efficiency of different LDOs.

2.3.9.2 Buck

The main parameters of the buck converter that affect the total estimated battery life are:

- The output voltage: $V_{out} = 3\text{ V}$
- The output on-current: $I_{on} = 9.1\text{ mA}$
- The output off-current: $I_{off} = 5\text{ }\mu\text{A}$
- The efficiency at the on-current: $\eta_{on} = 91\%$ (taken from the TPS62745 datasheet)
- The efficiency at the off-current: $\eta_{off} = 80\%$ (taken from the TPS62745 datasheet)
- The on-duty cycle: $D_{on} = t_{on} / T = 5\text{ ms} / 500\text{ ms} = 1\%$
- The off-duty cycle: $D_{off} = 1 - D_{on} = 99\%$

Equation 3 describes the average power loss of the buck converter during operation.

$$P_{Buck} = \left(\frac{1}{\eta_{on}} - 1\right) \times (V_{out}) \times (I_{on}) \times (D_{on}) + \left(\frac{1}{\eta_{off}} - 1\right) \times (V_{out}) \times (I_{off}) \times (D_{off})$$

$$P_{Buck} = \left(\frac{1}{0.91} - 1\right) \times (3\text{ V}) \times (9.1\text{ mA}) \times (0.01) + \left(\frac{1}{0.8} - 1\right) \times (3\text{ V}) \times (5\text{ }\mu\text{A}) \times (0.99) = 30.7\text{ }\mu\text{W} \tag{3}$$

Users can already see that the average power loss in the buck converter is an order of magnitude less than the LDO. The biggest differentiation in buck converters is the efficiency at both current loads, especially at the lighter load of 5 μA . Most converters are not as efficient at these lighter loads. The TPS62745 is a highly efficient buck converter, the reason for the choice. The majority of buck converters give their efficiency values on a curve as shown in Figure 13.

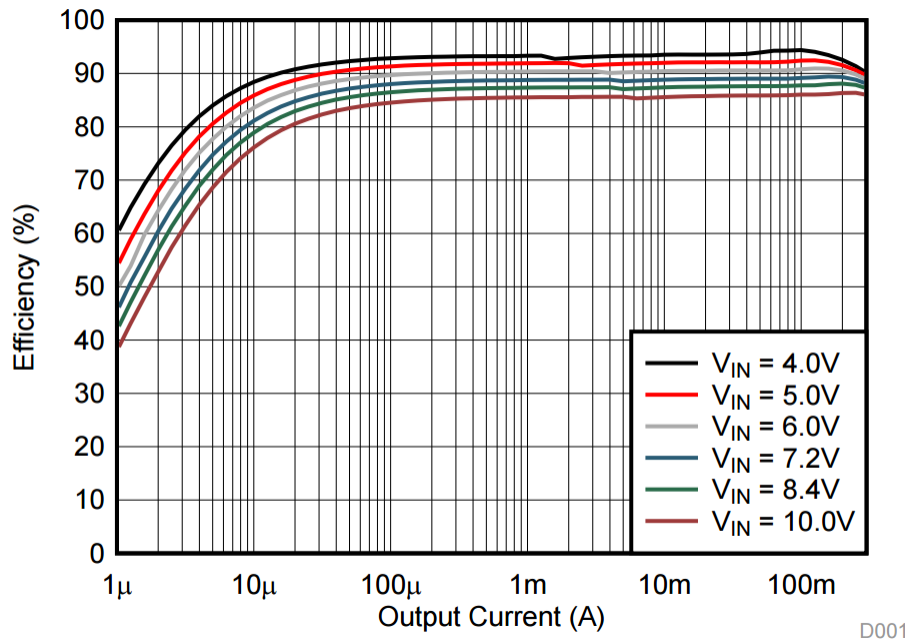


Figure 13. TPS62745 Efficiency Curve at $V_{OUT} = 3.3\text{ V}$

2.3.9.3 Boost

The main parameters of the boost converter that affect the total estimated battery life are:

- The output voltage: $V_{out} = 5\text{ V}$
- The average output motor current 1: $I_{out1} = 600\text{ mA}$
- The average output motor current 2: $I_{out2} = 168\text{ mA}$
- The efficiency at I_{out1} : $\eta_1 = 90\%$ (this value could be lower depending on the boost device)
- The efficiency at I_{out2} : $\eta_2 = 85\%$ (this value could be lower depending on the boost device)
- The average number of damper adjustment events per day: $N = 24$ (this number can vary)
- The on-time of I_{out1} : $t_{on1} = 2$ seconds (the time when the motor begins to turn)
- The on-time of I_{out2} : $t_{on2} = 4$ seconds (the time when braking and reconfiguring the direction of the motor)
- The total period in a day: $T = (3600) \times (24) = 86,400$ seconds

Equation 4 describes the average power loss of the boost converter during operation.

$$P_{Boost} = \left(\frac{1}{\eta_1} - 1\right) \times (V_{out}) \times (I_{out1}) \times \left(\frac{t_{on1} \times (N)}{T}\right) + \left(\frac{1}{\eta_2} - 1\right) \times (V_{out}) \times (I_{out2}) \times \left(\frac{t_{on2} \times (N)}{T}\right)$$

$$P_{Boost} = \left(\frac{1}{0.9} - 1\right) \times (5\text{ V}) \times (600\text{ mA}) \times \left(\frac{(2) \times (24)}{86400}\right) + \left(\frac{1}{0.85} - 1\right) \times (5\text{ V}) \times (168\text{ mA}) \times \left(\frac{(4) \times (24)}{86400}\right) = 349.9\text{ }\mu\text{W}$$
(4)

The boost configuration is highly dependent on the number of adjustment events (N), which occur per day as seen in Equation 4. As the number of adjustment events are decreased to 12 (half of 24), the power losses are also cut in half. Because the number of events is directly proportional with power losses, an unfavorable result, the boost is not preferred in a smart damper design when stepping up from 5 to 6 V and from 2.5 to 3 V.

2.3.9.4 Power Budget of All Three Power Topologies

The buck converter is by far the topology of choice for this TI Design. Because the majority of the power consumed and lost is in the three main devices (Bluetooth low energy or MCU, power regulator, and motor drive), Figure 14 shows these three and the percentages of how much power is used. The motor driver power consumption and losses are in Section 2.3.10, but the values are included for visual representation. The PFET for reverse polarity protection is not included in the pie chart because it consumes less than 1% of the total power in all of the following cases. The number of events is 24 for all pie charts. Figure 14 shows the Bluetooth low energy connection period at 500 ms, while Figure 15 shows the Bluetooth low energy connection period at 220 ms (this connection period is sometimes used in different applications like the Apple® HomeKit™).

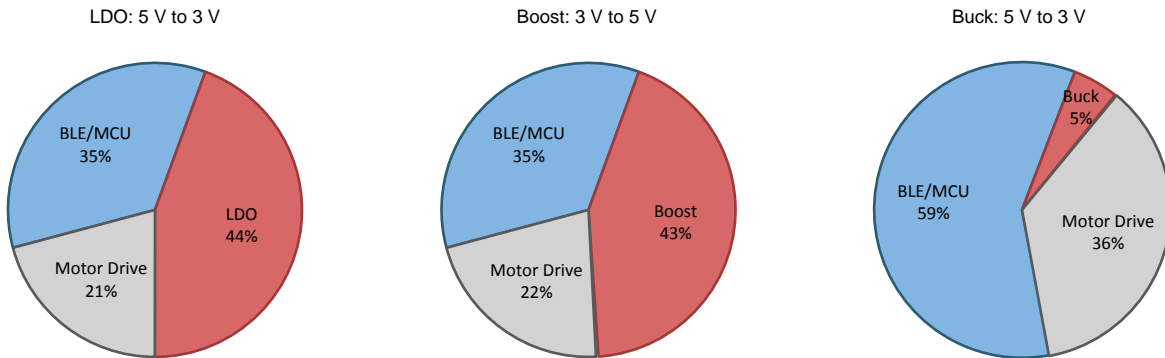


Figure 14. Power Consumption With 500-ms Bluetooth Low Energy Connection Period, Using 24 Adjustment Events

With a 500-ms connection period, the system is sleeping or off most of the time. The LDO and boost power configurations take up a significant amount of power (almost half in both cases) compared to the buck configuration, just 6%. Increasing the connection event period (this is an increase in duty cycle) to 220 ms (see Figure 15), shows similar results. In this case, the Bluetooth low energy or MCU consumes more power. The buck configuration is the most ideal power topology by far, as seen in Figure 14 and Figure 15.

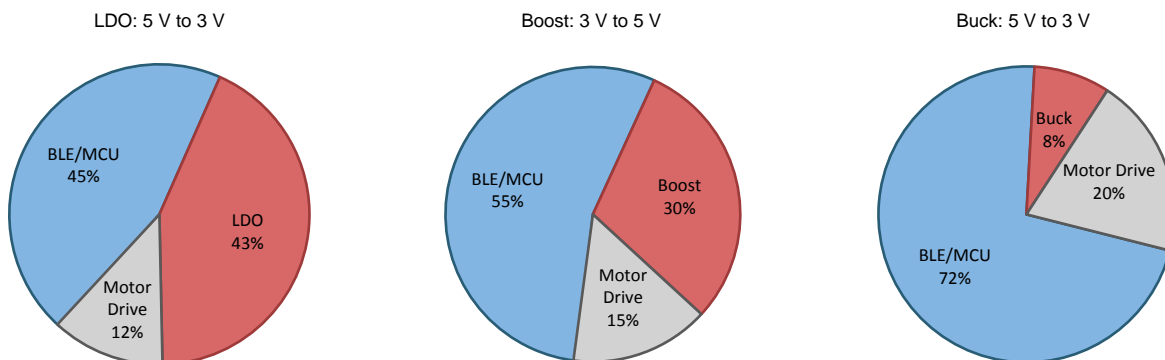


Figure 15. Power Consumption With 220-ms Bluetooth Low Energy Connection Period, Using 24 Adjustment Events

2.3.9.5 Battery Life Versus Number of Louver Adjustment Events of All Three Power Topologies

The following plots show the battery life, in months, versus the number of louver adjustment events per day. The plots provide a better visual representation of why the buck converter is the power topology of choice for battery life. The power dissipation of all the ICs (Bluetooth low energy or MCU, PFET, motor driver, and power) are included in the following graphs. The equations used in [Section 2.3.9](#) were incorporated into all the graphs. [Figure 16](#) shows the battery life with a 500-ms Bluetooth low energy connection period, whereas [Figure 17](#) shows the battery life with a 220-ms Bluetooth low energy connection period.

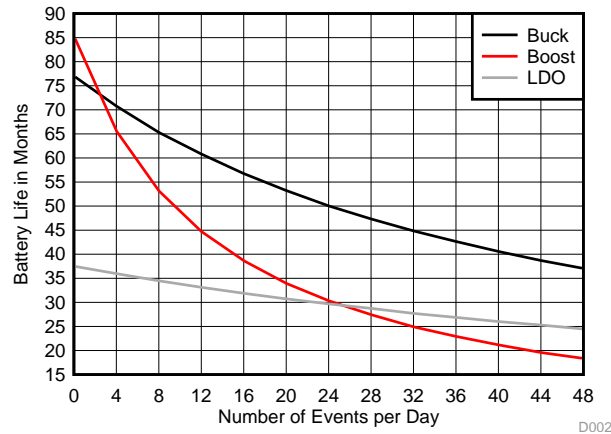


Figure 16. Number of Events Versus Battery Life With 500-ms Bluetooth Low Energy Connections

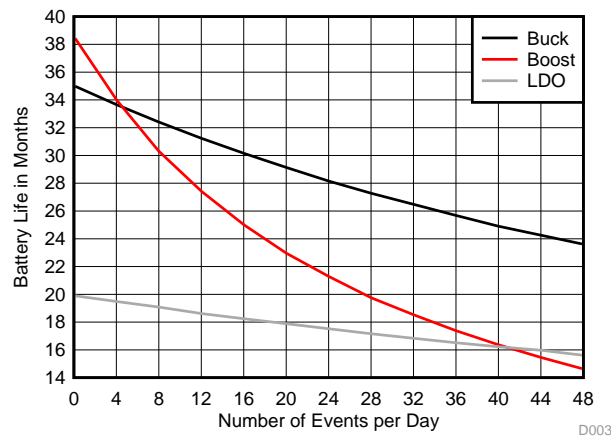


Figure 17. Number of Events Versus Battery Life With 220-ms Bluetooth Low Energy Connections

Another method to extend battery life is to extend the Bluetooth low energy connection period. The CC2650 can be programmed to extend the connection period from 10 ms to 4 seconds. Some products, like the Apple HomeKit, have strict connection specifications. [Figure 18](#) shows the battery life versus the period of Bluetooth low energy connections using 12 adjustment events, whereas [Figure 19](#) shows the same graph, but this time using 24 adjustment events. With the increase of louver rotation adjustment events, the buck topology becomes more advantageous than the other power topologies, as seen in [Figure 19](#).

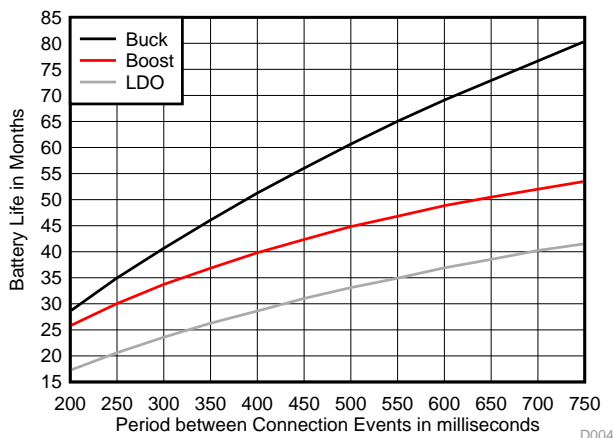


Figure 18. Bluetooth Low Energy Connection Period Versus Battery Life With 12 Events

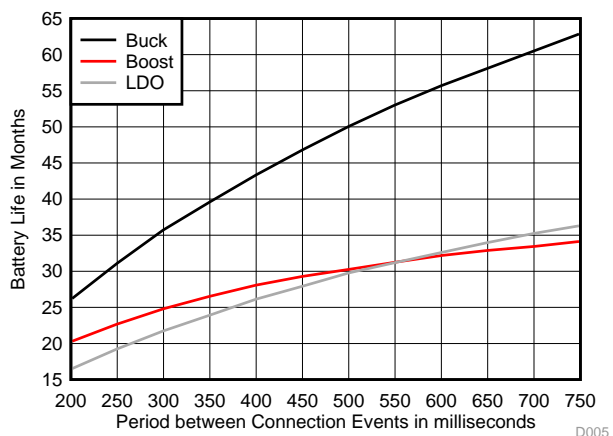


Figure 19. Bluetooth Low Energy Connection Period Versus Battery Life With 24 Events

2.3.10 Motor Driver Average Power Consumption

A number of sources of power dissipation exist inside a motor driver IC. To make an accurate assessment of the total power dissipation, all sources must be considered. The motor driver in this TI Design (DRV8833) has a current-sense pin that limits the amount of the current through the H-bridge and motor. The sense resistor also dissipates power on top of the other sources. In all, there are four sources of power dissipation in a motor driver application (more exist, but the power dissipated in them is negligible and therefore does not make a significant difference in the overall equation). For a more in-depth explanation on calculating motor driver power dissipation, see the application report [Calculating Motor Driver Power Dissipation](#) (SLVA504).

2.3.10.1 R_{DSon} Dissipation

The biggest source of power dissipated inside a motor driver device is the power dissipated in the FET on resistance, R_{DSon} . Similar to the boost power topology section, two current scenarios are at play: when the motor begins to turn and when it is coasting and braking.

The main parameters of R_{DSon} dissipation that affect the total estimated battery life are as follows:

- The on-resistance of the H-bridge FETs: $R_{DSon} = 360 \text{ m}\Omega$ (DRV8833 datasheet)
- The root mean square current 1: $I_{RMS1} = 447 \text{ mA}$ (this is different from average current)
- The root mean square current 2: $I_{RMS2} = 140 \text{ mA}$

Equation 5 shows the power dissipated through the on-resistance of the FETs during operation.

$$P_{Rds1} = (R_{DSon}) \times (I_{RMS1})^2$$

$$P_{Rds1} = (360 \text{ m}\Omega) \times (0.447 \text{ A})^2 = 71.93 \text{ mW}$$

$$P_{Rds2} = (R_{DSon}) \times (I_{RMS2})^2$$

$$P_{Rds2} = (360 \text{ m}\Omega) \times (0.14 \text{ A})^2 = 7.06 \text{ mW} \quad (5)$$

2.3.10.2 Switching Losses

The main parameters of switching losses that affect the total estimated battery life are as follows:

- The supply voltage: $V_M = 5 \text{ V}$
- The average output motor current 1: $I_{M1} = 600 \text{ mA}$
- The average output motor current 2: $I_{M2} = 168 \text{ mA}$
- The frequency that the output is switching: $f_{sw} = 50 \text{ kHz}$ (DRV8833 datasheet)
- The rise and fall times of the output: $t_{rise} + t_{fall} = 340 \text{ ns}$ (DRV8833 datasheet)

Equation 6 shows the switching losses of the H-bridge FETs during operation.

$$P_{SW1} = (1/2) \times (V_M) \times (I_{M1}) \times (f_{SW}) \times (t_{rise} + t_{fall})$$

$$P_{SW1} = (1/2) \times (5 \text{ V}) \times (600 \text{ mA}) \times (50 \text{ kHz}) \times (340 \text{ ns}) = 25.5 \text{ mW}$$

$$P_{SW2} = (1/2) \times (V_M) \times (I_{M2}) \times (f_{SW}) \times (t_{rise} + t_{fall})$$

$$P_{SW2} = (1/2) \times (5 \text{ V}) \times (168 \text{ mA}) \times (50 \text{ kHz}) \times (340 \text{ ns}) = 7.14 \text{ mW} \quad (6)$$

2.3.10.3 Operating Supply Current

The main parameters of the operating supply current that affect the total estimated battery life are as follows:

- The supply voltage: $V_M = 5 \text{ V}$
- The supply current: $I_M = 1.7 \text{ mA}$ (DRV8833 datasheet)
- The sleep current: $I_{MQ} = 1.6 \mu\text{A}$ (DRV8833 datasheet)

Equation 7 shows the power consumed through the motor drive device.

$$P_M = (V_M) \times (I_M)$$

$$P_M = (5 \text{ V}) \times (1.7 \text{ mA}) = 8.5 \text{ mW}$$

$$P_{MQ} = (V_M) \times (I_{MQ})$$

$$P_{MQ} = (5 \text{ V}) \times (1.6 \mu\text{A}) = 8.0 \mu\text{W} \quad (7)$$

2.3.10.4 Sense Resistor Dissipation

The sense resistor is used for current regulation. The maximum trip current is set according to the equation in the DRV8833 datasheet. The main parameters of sense resistor power dissipation that affect the total estimated battery life are as follows:

- The sense resistor: $R_{\text{sen}} = 100 \text{ m}\Omega$
- The root mean square current 1: $I_{\text{RMS1}} = 447 \text{ mA}$ (this is different from average current)
- The root mean square current 2: $I_{\text{RMS2}} = 140 \text{ mA}$

Equation 8 shows the power dissipated through the sense resistor during operation.

$$P_{\text{sen1}} = (R_{\text{DSon}}) \times (I_{\text{RMS1}})^2$$

$$P_{\text{sen1}} = (100 \text{ m}\Omega) \times (0.447 \text{ A}) = 19.98 \text{ mW}$$

$$P_{\text{sen2}} = (R_{\text{DSon}}) \times (I_{\text{RMS2}})^2$$

$$P_{\text{sen2}} = (100 \text{ m}\Omega) \times (0.14 \text{ A}) = 1.96 \text{ mW}$$

(8)

2.3.10.5 Total Average Power Dissipation

There are two H-bridges in the DRV8833, each connected in parallel to the brushed DC motor. Because of these H-bridges, there is a factor of 2 on the R_{DSon} dissipation and switching losses component of the overall motor driver system. The main parameters of the overall motor driver power dissipation that affect the total estimated battery life are as follows:

- The on-time 1: $t_{\text{on1}} = 2$ seconds (the time when the motor begins to turn)
- The on-time 2: $t_{\text{on2}} = 4$ seconds (the time spent braking, coasting, and reconfiguring the direction of the motor)
- The average number of adjustment events per day: $N = 24$ (this number can vary)
- The total period in a day: $T = (3600) \times (24) = 86,400$ seconds

Equation 9 shows the average power dissipation in the motor driver overall during operation.

$$P_{\text{MD}} = (2 \times P_{\text{Rds1}} + 2 \times P_{\text{SW1}} + P_{\text{M}} + P_{\text{sen1}}) \times \left(\frac{t_{\text{on1}} \times (N)}{T} \right) + (2 \times P_{\text{Rds2}} + 2 \times P_{\text{SW2}} + P_{\text{M}} + P_{\text{sen2}}) \times \left(\frac{t_{\text{on2}} \times (N)}{T} \right) + P_{\text{MQ}}$$

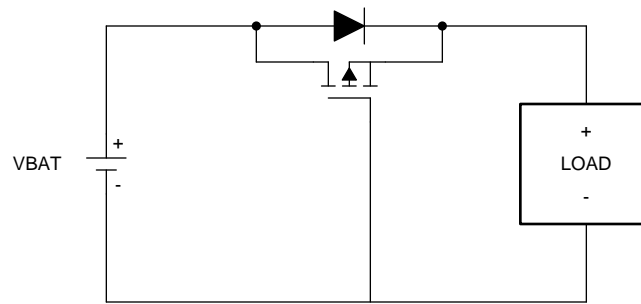
$$P_{\text{MD}} = (2 \times 71.93 \text{ mW} + 2 \times 25.5 \text{ mW} + 8.5 \text{ mW} + 19.98 \text{ mW}) \times \left(\frac{(2) \times (24)}{86400} \right) + (2 \times 7.06 \text{ mW} + 2 \times 7.14 \text{ mW} + 8.5 \text{ mW} + 1.99 \text{ mW}) \times \left(\frac{(4) \times (24)}{86400} \right) + 8 \mu\text{W} = 175.26 \mu\text{W}$$

(9)

The power dissipation on the motor drive device is almost directly proportional to the number of rotary adjustment events. Besides using all of the previous equations, a plot of battery life versus the number of events is shown in Section 2.3.13 to quickly calculate the estimated battery life in months. The experimental average current values are discussed in Section 4.2.

2.3.11 Reverse Polarity Protection Power Consumption of PFET

Any system that is powered by batteries must have some kind of safeguard in case of reverse battery installation. If reverse battery installation occurs, there could be serious damage to the internal electronics without a reverse polarity protection circuit. In the theme of ultra-low-power consumption, this TI Design has a PFET, instead of a diode, for its very low on-resistance and drop-in voltage. The reason for using a PFET instead of a NFET is to prevent breaking the ground plane. The NFET is in the ground return path while the PFET is in the power path. [Figure 20](#) shows how the PFET is wired in the overall circuit.



Copyright © 2016, Texas Instruments Incorporated

Figure 20. Reverse Polarity Protection PFET Configuration

In the circuit in [Figure 20](#), the body diode of the PFET is oriented in the direction of normal current flow. When the battery is installed incorrectly, the gate voltage of the PFET is high, preventing it from turning on. When the battery is installed properly, the gate voltage of the PFET is taken low, and its channel shorts out the diode.

The most important parameter to consider when choosing a PFET is the value of the R_{DSon} (lower is better). The value of the gate charge is not important because this application does not use the PFET as a switching component, and therefore does not have switching losses. The main parameters of the PFET that affect the total estimated battery life are as follows:

- The on-resistance of the PFET: $R_{DSon} = 18 \text{ m}\Omega$ (CSD25310Q2 datasheet)
- The output on current through the PFET: $I_{on} = 6 \text{ mA}$ (current in from battery-to-buck converter)
- The output off current through the PFET: $I_{off} = 3.75 \text{ }\mu\text{A}$ (current in from battery-to-buck converter)

The remainder of the parameters are the same as those previously discussed:

- The on-duty cycle: $D_{on} = t_{on} / T = 5 \text{ ms} / 500 \text{ ms} = 1\%$
- The off-duty cycle: $D_{off} = 1 - D_{on} = 99\%$
- The average output motor current 1: $I_{out1} = 600 \text{ mA}$
- The average output motor current 2: $I_{out2} = 168 \text{ mA}$
- The on-time 1: $t_{on1} = 2 \text{ seconds}$ (time when the motor begins to turn)
- The on-time 2: $t_{on2} = 4 \text{ seconds}$ (time spent braking, coasting, and reconfiguring direction of the motor)
- The average number of louver adjustment events per day: $N = 24$ (this number can vary)
- The total period in a day: $T = (3600) \times (24) = 86,400 \text{ seconds}$

[Equation 10](#) shows the average power dissipation in the PFET during operation.

$$P_{PFET} = (R_{DSon}) \times (I_{on})^2 \times (D_{on}) + (R_{DSon}) \times (I_{off})^2 \times (D_{off}) + (R_{DSon}) \times (I_{out1})^2 \times \left(\frac{t_{on1} \times (N)}{T}\right) + (R_{DSon}) \times (I_{out2})^2 \times \left(\frac{t_{on2} \times (N)}{T}\right)$$

$$P_{PFET} = (18 \text{ m}\Omega) \times (6 \text{ mA})^2 \times (0.01) + (18 \text{ m}\Omega) \times (3.75 \text{ }\mu\text{A})^2 \times (0.99) + (18 \text{ m}\Omega) \times (600 \text{ mA})^2 \times \left(\frac{(2) \times (24)}{86400}\right) + (18 \text{ m}\Omega) \times (168 \text{ mA})^2 \times \left(\frac{(4) \times (24)}{86400}\right) = 4.17 \text{ }\mu\text{W} \quad (10)$$

The current coming in from the battery (I_{on} and I_{off}) was calculated by using the efficiency of the buck converter and then back calculating the input power, hence the input current (5 V is the nominal battery voltage). Looking at the value in [Equation 10](#), $4.17 \text{ }\mu\text{W}$ is less than 1% of the total power consumed and lost in this TI Design. The PFET makes an insignificant difference in the overall power budget and battery life.

2.3.12 Total System Power Consumption

To calculate the total system average power consumption, simply add all average power values from each device from the previous sections (minus the LDO and boost). [Equation 11](#) reflects this combination and shows the total system average power dissipation during operation.

$$P_{\text{avg}} = P_{\text{BLE}} + P_{\text{Buck}} + P_{\text{MD}} + P_{\text{PFET}}$$

$$P_{\text{avg}} = 280.4 \mu\text{W} + 30.7 \mu\text{W} + 175.26 \mu\text{W} + 4.17 \mu\text{W} = 490.53 \mu\text{W} \text{ (total average power)} \quad (11)$$

As stated in the beginning of this design guide, these equations only cover the core of any smart damper design. If more peripherals are added to this system, calculate the average power consumed by each extra peripheral by using similar previous methods. For example, determining the duty cycle, calculating the on- and off-current consumption per peripheral, and so on.

2.3.13 Theoretical Estimated Battery Life

The majority of batteries show their capacity measured in milliamp-hours (mAh). The mAh is a measure of current capacity and not really energy capacity (but they are closely related). A better unit for measuring energy capacity of a battery is in mWh. To convert the mAh capacity of a battery to mWh, first look at the battery datasheet.

Take the AA Energizer® battery for example, as shown in Figure 21.

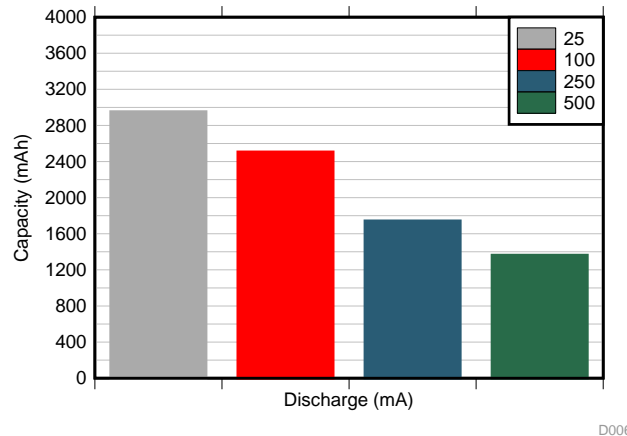


Figure 21. mAh Capacity of Energizer AA Battery

Calculate the average discharge current in your smart damper system. In this case, the average load current is much less than 25 mA, so look at the capacity at that value (which is the lowest value on the battery datasheet). Then use these parameters to figure out the values needed for total energy capacity of the batteries:

- The battery current capacity of one cell: $I_{energy} = 3000 \text{ mAh}$ (alkaline AA battery datasheet)
- The number of batteries configured in parallel: $Batt_{||} = 1$ (all four batteries are in series: 4s1p)
- The number of batteries configured in series: $Batt_{series} = 4$
- The starting voltage of one battery cell: $V_{batt} = 1.5 \text{ V}$ (one alkaline AA battery)

See Equation 12 to convert the batteries current capacity, mAh, into mWh.

$$E_{total} = (I_{energy}) \times (Batt_{||}) \times (V_{batt}) \times (Batt_{series})$$

$$E_{total} = (3,000 \text{ mA} \cdot \text{h}) \times (1) \times (1.5 \text{ V}) \times (4) = 18,000 \text{ mW} \cdot \text{hours} \tag{12}$$

Lastly, the amount of battery life in hours can be calculated by using the equations in Equation 11 for average power of the system and Equation 12 for total energy capacity of the battery.

Equation 13 shows the number of months of battery life during operation.

$$\text{Months} = \left(\frac{E_{total}}{P_{avg}} \right) \times \left(\frac{1 \text{ day}}{24 \text{ hours}} \right) \times \left(\frac{1 \text{ month}}{30.5 \text{ days}} \right)$$

$$\text{Months} = \left(\frac{18,000 \text{ mW} \cdot \text{hours}}{0.49053 \text{ mW}} \right) \times \left(\frac{1 \text{ day}}{24 \text{ hours}} \right) \times \left(\frac{1 \text{ month}}{30.5 \text{ days}} \right) = 50.1 \text{ months of battery life (5 years)} \tag{13}$$

The final plot shows the battery life, in months, versus the number of adjustment events per day using just the buck topology, which is the power topology of choice for this reference design. The plot, shown in [Figure 22](#), shows four different Bluetooth low energy connection event periods on the same graph: 220 ms, 360 ms, 500 ms, and 640 ms. The power dissipation of all ICs (Bluetooth low energy or MCU, PFET, motor driver, and power) is included in this MATLAB graph. The equations used in [Section 2.3](#) were incorporated into all the graphs.

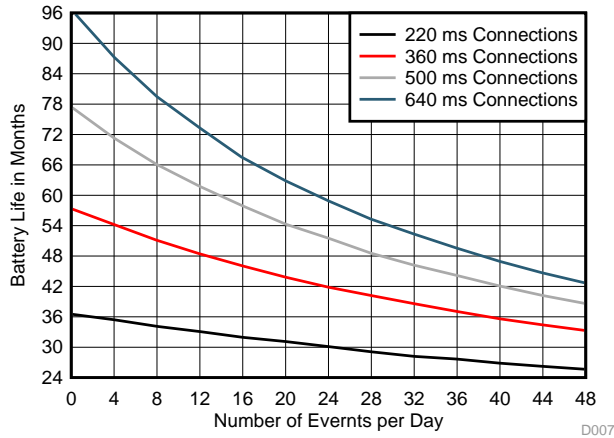


Figure 22. Number of Events Versus Battery Life With Buck Converter

2.3.14 Firmware Control

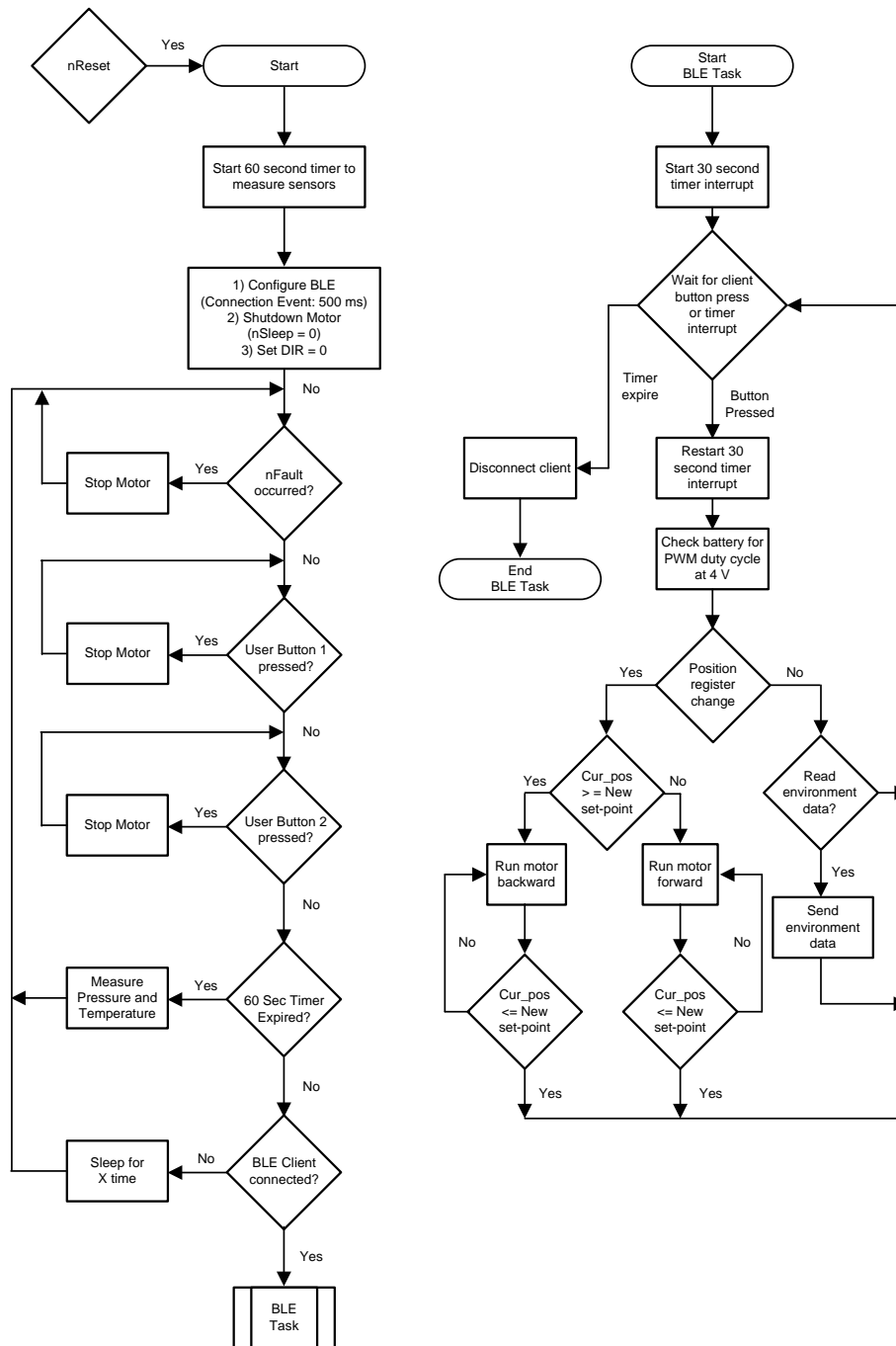


Figure 23. Software Flow Chart

This flow chart shown in [Figure 23](#) describes the CC2650 operation in this TI Design. The CC2650 starts by initializing the timer to schedule the environment sensing and configuring the DRV8833 devices to its lowest power state. Afterward, the CC2650 advertises with a 500-ms interval. The CC2650 also monitors the battery voltage in one-hour intervals while it is waiting for a device to connect. The main loop of the CC2650 is event based. The majority of the time, the CC2650 is in standby mode, except when it must transmit an advertisement packet, measure environmental sensors or check the battery voltage. When an event is triggered, the CC2650 wakes up and executes functions depending on the event source.

The CC2650 has six event triggers:

- **GAP role state change event:** This event occurs when the GAP role state changes (for example, when a device connects or disconnects from the CC2650). When a device connects to the CC2650, the current load changes. The voltage-based battery monitoring does not give an accurate representation of the battery voltage, because the measured voltage is a function of the battery impedance and the load current. Also, for security and battery savings, a device must not be connected indefinitely. In this firmware, the device is automatically disconnected after 30 seconds of inactivity. When a device connects, the battery monitor is stopped and the inactivity timer is started immediately. When a device disconnects (either by the user or by the inactivity time-out), the battery monitoring resumes.
- **Attribute value change event:** This event occurs when the user changes the louver rotary position. The CC2650 first starts by verifying whether the new value is valid. If the new value is not valid, then the value is discarded and no action is taken. If the new value is valid, the new position is saved and the inactivity timer is restarted. Next, the battery voltage is read to calculate the correct PWM duty cycle to run the motor at 4 V. If the new value is greater than the current position read by the rotary potentiometer sensor, the motor drives backward while the potentiometer is checked every 10 ms to see if the position is close to the desired position. If the new value is less than the current position, the motor drives forward until the potentiometer position sensor verifies the correct position.
- **Inactivity time-out event:** If the 30 second inactivity time-out expires, the CC2650 disconnects the device and returns to the advertising. When this event occurs, the CC2650 also triggers a GAP role state change event.
- **Test button pressed event:** The test buttons are valid only when a device is not connected. If a device is connected, the test buttons are ignored, so the device does not interfere with the user's operation. If user button *one* is pressed, the "louver" is moved to the fully open position. If user button *two* is pressed, the CC2650 drives the motor to the fully open position.
- **Battery monitor event:** This event is the 1 hour battery monitor periodic event. The C2650 reads the current battery voltage.
- **The DRV8833 fault occur event:** If the DRV8833 fault pin indicates an error occurred when running the motor. The current implementation of the firmware doesn't do anything with this error. The firmware can be modified to rerun the motor until it can successfully move the louver without an error. In addition, the firmware contains a GATT server with the following services:
 - GAP
 - GATT
 - Device information
 - Rotary position
 - Temperature (°C)
 - Humidity (%)
 - Pressure (hPA)

Device information service is aligned to official SIG profiles. The smart damper profile is a custom profile with 128-bit unique UUIDs. The profile enables a device to configure the rotary position of the TIDA-01067 TI Design. The complete attribute table for TIDA-01067 is shown in [Table 2](#).

Table 2. TIDA-01067 Attribute Table

HANDLE (HEX)	HANDLE (DEC)	TYPE (HEX)	TYPE (TEXT)	HEX VALUE	GATT SERVER PERMISSIONS	DESCRIPTION AND VALUE (TEXT)
0x1	1	0x2800	GATT Primary Service Declaration	0x1800	R	Generic access service
0x2	2	0x2803	GATT Characteristic Declaration	02:03:00:00:2A	R	Device name
0x3	3	0x2A00	Device Name	—	R	—
0x4	4	0x2803	GATT Characteristic Declaration	02:05:00:01:2A	R	Appearance
0x5	5	0x2A01	Appearance	—	R	—
0x6	6	0x2803	GATT Characteristic Declaration	02:07:00:04:2A	R	Peripheral preferred connection parameters
0x7	7	0x2A04	Peripheral Preferred Connection Parameters	—	R	—
0x8	8	0x2800	GATT Primary Service Declaration	0x1801	R	Generic attribute service
0x9	9	0x2800	GATT Primary Service Declaration	0x180A	R	Device information service
0xA	10	0x2803	GATT Characteristic Declaration	02:0B:00:23:2A	R	System ID
0xB	11	0x2A23	System ID	86:56:74:00:00:F8:E6:A0	R	—
0xC	12	0x2803	GATT Characteristic Declaration	02:0D:00:24:2A	R	Model number string
0xD	13	0x2A24	Model Number String	54:49:44:41:2D:30:30:37:35:37:20:54:49:20:44:65:73:69:67:6E	R	TIDA-01067 TI Design
0xE	14	0x2803	GATT Characteristic Declaration	02:0F:00:25:2A	R	Serial number string
0xF	15	0x2A25	Serial Number String	53:65:72:69:61:6C:20:4E:75:6D:62:65:72	R	Serial number
0x10	16	0x2803	GATT Characteristic Declaration	02:11:00:26:2A	R	Firmware revision string
0x11	17	0x2A26	Firmware Revision String	46:69:72:6D:77:61:72:65:20:52:65:76:3A:20:31:2E:30	R	Firmware rev: 1.0
0x12	18	0x2803	GATT Characteristic Declaration	02:13:00:27:2A	R	Hardware revision string
0x13	19	0x2A27	Hardware Revision String	48:61:72:64:77:61:72:65:20:52:65:76:3A:20:31:2E:30	R	Hardware rev: 1.0

Table 2. TIDA-01067 Attribute Table (continued)

HANDLE (HEX)	HANDLE (DEC)	TYPE (HEX)	TYPE (TEXT)	HEX VALUE	GATT SERVER PERMISSIONS	DESCRIPTION AND VALUE (TEXT)
0x14	20	0x2803	GATT Characteristic Declaration	02:15:00:28:2A	R	Software revision string
0x15	21	0x2A28	Software Revision String	53:6F:66:74:77:61:72:65:20:52:65:76:3A:20:31:2E:30	R	Software rev: 1.0
0x16	22	0x2803	GATT Characteristic Declaration	02:17:00:29:2A	R	Manufacturer name string
0x17	23	0x2A29	Manufacturer Name String	54:65:78:61:73:20:49:6E:73:74:72:75:6D:65:6E:74:73	R	Texas Instruments
0x18	24	0x2803	GATT Characteristic Declaration	02:19:00:2A:2A	R	IEEE 11073-20601 Regulatory Certification Data List
0x19	25	0x2A2A	IEEE 11073-20601 Regulatory Certification Data List	FE:00:65:78:70:65:72:69:6D:65:6E:74: 61:6C	R	Experimental
0x1A	26	0x2803	GATT Characteristic Declaration	02:1B:00:50:2A	R	PnP ID
0x1B	27	0x2A50	PnP ID	01:0D:00:00:00:10:01	R	—
0x1C	28	0x2800	GATT Primary Service Declaration	F0007570-0451-4000-B000-000000000000	R	Smart Vent service
0x1D	29	0x2803	GATT Characteristic Declaration	0E:1E:00:00:00:00:00:00:00:00:00:00:00:40:51:04:71:75:00:F0	R	Vent Pos.
0x1E	30	0x7571	Vent State Config	03	RW	Write 0 to close, 6 to fully close, any number in between to set position
0x1F	31	0x2901	Characteristic User Description	56:65:6E:74:20:50:6F:73:2E:20:28:30:3A:63:6C:6F:73:65:20:2D:20:36	R	Vent Pos. (0:Close - 6:open)
0x20	32	0x2803	GATT Characteristic Declaration	12:21:00:00:00:00:00:00:00:00:00:00:00:40:51:04:75:75:00:F0	R	—
0x21	33	0x7575	Temperature	00	R/N	—
0x22	34	0x2902	Client Characteristic Configuration	00:00	RW	Write "01:00" to enable notifications, "00:00" to disable
0x23	35	0x2901	Characteristic User Description	54:65:6D:70:65:72:61:74:75:72:65:20:43	R	Temperature C
0x24	36	0x2803	GATT Characteristic Declaration	12:25:00:00:00:00:00:00:00:00:00:00:00:40:51:04:76:75:00:F0	R	—
0x25	37	0x7576	Humidity %	00	R/N	—
0x26	38	0x2902	Client Characteristic Configuration	00:00	RW	Write "01:00" to enable notifications, "00:00" to disable
0x27	39	0x2901	Characteristic User Description	48:75:6D:69:64:69:74:79:20:25	R	Humidity %

Table 2. TIDA-01067 Attribute Table (continued)

HANDLE (HEX)	HANDLE (DEC)	TYPE (HEX)	TYPE (TEXT)	HEX VALUE	GATT SERVER PERMISSIONS	DESCRIPTION AND VALUE (TEXT)
0x28	40	0x2803	GATT Characteristic Declaration	12:29:00:00:00:00:00:00:00:00:B0:00:40:51:04:77:75:00:F0	R	—
0x29	41	0x7576	Pressure	00:00	R/N	—
0x2A	42	0x2902	Client Characteristic Configuration	00:00	RW	Write "01:00" to enable notifications, "00:00" to disable
0x2B	43	0x2901	Characteristic User Description	50:72:65:73:73:75:72:65:20:28:68:50:61:29	R	Pressure (hPa)

3 Getting Started Hardware and Firmware

This section provides an overview describing how to get started with the EVM hardware and software.

3.1 Getting Started Hardware

3.1.1 Hardware Overview

Figure 24 shows the hardware for the TIDA-01067 reference design. The PCB is in a 3.5-in×4.0-in rectangular form factor. However, no steps were taken to shrink down the form factor during development. The PCB sits on 1.25-in nylon standoffs to enable ease of use while performing lab measurements.

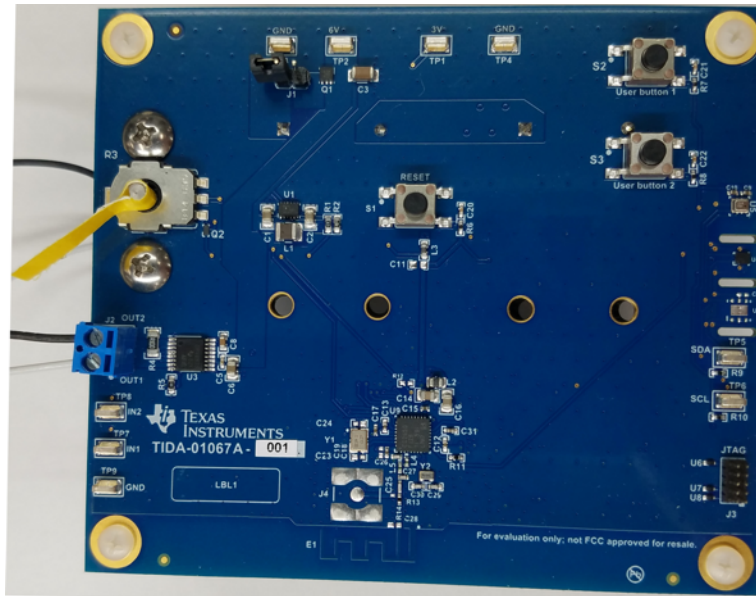


Figure 24. Smart Damper Reference Design Hardware

The jumper J1 in the top left corner of the board lets the user disconnect the batteries from the rest of the reference design. J1 also enables collection of current measurements from the 6-V power rail. The lower left corner of the board contains the motor connection terminal block and test points along with the DRV8833 motor controller. I²C test points are on the lower right corner of the board next to the JTAG programming headers.

The CC2650 and PCB antenna are in the lower middle section of the board. This TI Design also includes a few push-buttons. Two user push-buttons are in the upper right corner, whereas the reset button is in the middle of the board.

3.1.2 Operating TIDA-01067 Design

TI recommends installing the batteries with J1 removed, and afterwards installing the jumper to power up the circuit. On power up, the motor will turn to the 50% open position to let the user know power up was successful.

When a device is not connected using Bluetooth the user buttons (S2 and S3) activate different features of the design. The louver moves to fully open position when S2 is pressed. S3 drives the motor to the fully closed position. To communicate using Bluetooth the iOS app called LightBlue™ was used for testing. Other generic Bluetooth apps can be used on various platforms. The B-BLE app on a Samsung® Galaxy S7® was tested for functionality. See Section 3.2.3 for further steps on running the firmware on this reference design.

3.2 Getting Started Firmware

3.2.1 Compiling Firmware

The firmware used for this TI Design was developed using TI's CCS software (version 6.1.0), BLE SDK 2.02.00.31, TI-RTOS 2.18.00.03 and ARM Compiler Tools 5.2.7. The instructions to build the firmware assume that CCS and the software packages have been set up and configured correctly. For more information on how to setup the development environment, consult the *CC2650 BLE Software Developer's Guide* provided in the docs folder of the BLE SDK.

To import the CCS project:

1. Open CCS.
2. Click on the *Project* toolbar.
3. Select *Import CCS Projects...*
4. Select the radio option *Select archive file*.
5. Navigate to where the *TIDA01067_BLE_Peripheral_Stack.zip* file is installed. If using the default location, the firmware is at folder location, *C:\ti\TIDA01067-Firmware*.
6. Verify that the option *TIDA01067_BLE_Peripheral_Stack* is checked.
7. Click the *Finish* button.
8. Repeat Steps 2 through 7 to import *TIDA01067_BLE_Peripheral_App*.

At this point, the CCS workspace should have both *TIDA01067_BLE_Peripheral_App* and *TIDA01067_BLE_Peripheral_Stack* projects.

To build the firmware:

1. Set the *TIDA01067_BLE_Peripheral_Stack* project as the active project, and build the project using *Project* → *Build Project*. The generated binary file, *TIDA067_BLE_Peripheral_Stack.hex*, is in the *TIDA01067_BLE_Peripheral_Stack/FlashROM* folder.
2. Set the *TIDA01067_BLE_Peripheral_App* project as the active project, and build the project using *Project* → *Build Project*. The generated binary file, *TIDA01067_BLE_Peripheral_App.hex*, is in the *TIDA01067_BLE_Peripheral_App/FlashROM* folder.

3.2.2 Loading Firmware

The TI Design hardware is programmed by connecting the 10-pin mini ribbon cable from J3 to the SmartRF06 EVM (10-pin ARM Cortex Debug Connector, P410). On the SmartRF06 EVM, set the source switch to *USB*, and short the *VDD to EM* jumper. In this configuration, the SmartRF06 EVM provides power to the CC2650. See the SmartRF06 EVM documentation for more information ([SWRU321](#)).

See [Figure 25](#) for the correct set up for connecting the TI Design hardware to the SmartRF06 EVM. Two applications can be used to program the TIDA-01067: Code Composer Studio or SmartRF Flash Programmer 2.

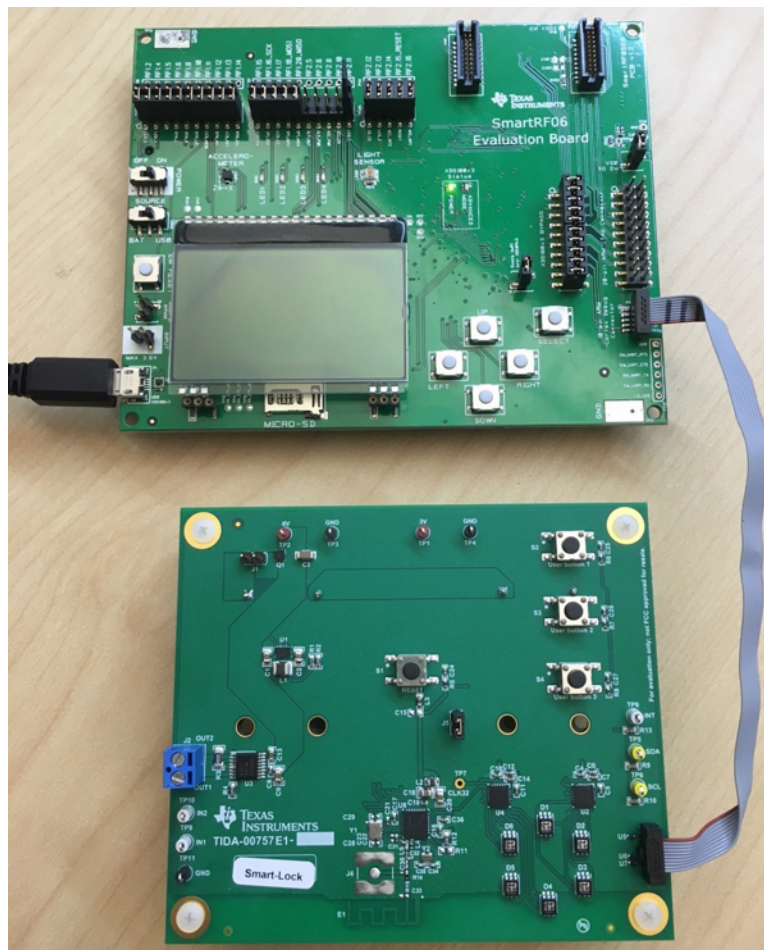


Figure 25. Connection of SmartRF06 Evaluation Board and TI Designs Hardware for Programming and Debugging

3.2.2.1 Programming With CCS

Perform the following steps to program with CCS:

1. Download *TIDA01067_BLE_Peripheral_Stack* by selecting the *TIDA01067_BLE_Peripheral_Stack* project as the active project, and choosing *Run* → *Debug*.
2. Choose *Run* → *Terminate* to stop the debug.
3. Download *TIDA001067_BLE_Peripheral_App* by selecting the *TIDA01067_BLE_Peripheral_App* project as the active project, and choosing *Run* → *Debug*.

NOTE: The preceding steps are needed only for the initial download, and whenever the Stack project is modified. As long as the Stack project is not modified, the only required steps are:

1. Build the application.
 2. Download the application.
-

3.2.2.2 Programming With SmartRF Flash Programmer 2

Perform the following steps to program with SmartRF Flash Programmer 2:

1. Download and install SmartRF Flash Programmer 2, available at: <http://www.ti.com/tool/flash-programmer>.
2. Open SmartRF Flash Programmer 2.
3. In the *Connected devices* window, CC2650 is listed under XDS100v3. If it is not listed, check the power and connection from SmartRF06 to TIDA-01067, and click the *Refresh* button to rescan for devices. Highlight the CC2650 device (see [Figure 26](#)).
4. In the *Main* tab, click the *Multiple* radio button.
5. Click the *Browse* button and navigate to the *TIDA001067 Stack hex file*.
6. Click the *Browse* button and navigate to the *TIDA01067 App hex file*.
7. Click the blue circle *Play* button to flash the two hex images onto the TIDA-01067.

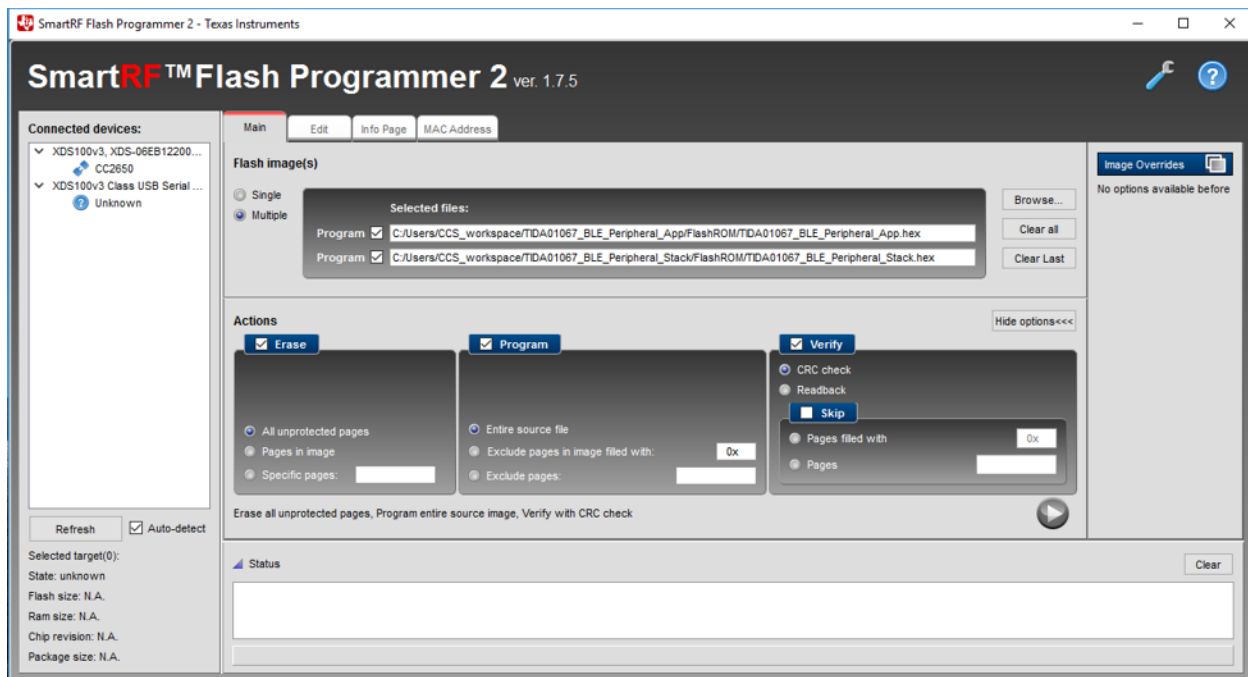


Figure 26. SmartRF Flash Programmer 2 Configuration

- The status bar at the bottom of the SmartRF Flash Programmer 2 shows whether flashing the images was successful (see [Figure 27](#)).

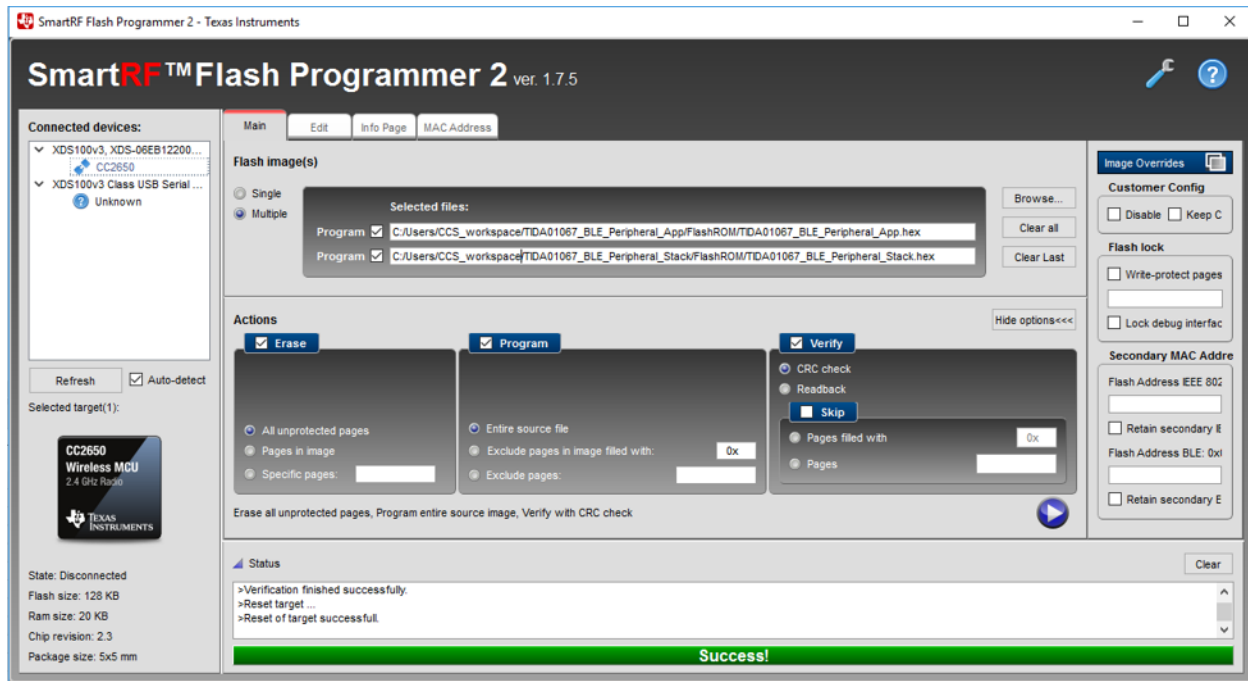


Figure 27. SmartRF Flash Programmer 2 Successful Flash Status

3.2.3 Running Firmware

To communicate with the TIDA-01067, an iPhone® 6 with the *LightBlue* iOS app is used for testing. A different platform or app can perform this function. The app *B-BLE* on the Samsung Galaxy S6 and S7 was tested for functionality.

- If not previously done, disconnect the SmartRF06 ribbon cable from the TIDA-01067.
- Remove J1 to disconnect the battery from the system.
- Insert four AA batteries into the battery holders or use a bench power supply.
- Power on the board by shunting J1 to connect the battery to the system.

NOTE: The motor will adjust the position of the louver to 50% open to indicate that the firmware is running.

- Enable Bluetooth on the iPhone.
- Run the LightBlue app.

- View the peripherals nearby (see [Figure 28](#)).

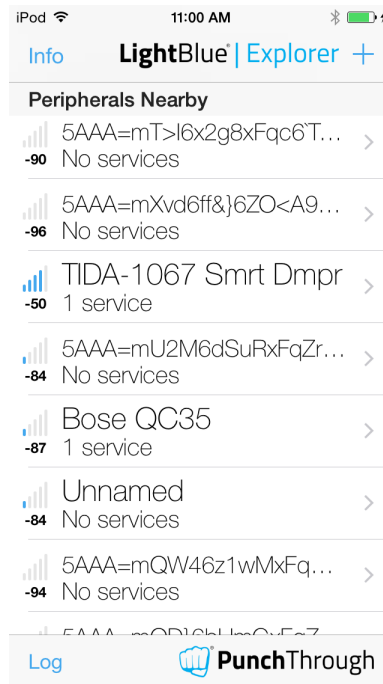


Figure 28. View Peripherals Screen

- Click the *TIDA-01067 Smrt Dmpr* peripheral to connect (see [Figure 29](#)).

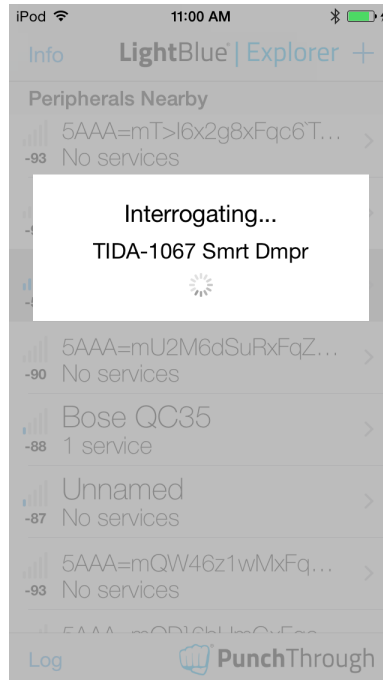


Figure 29. TIDA-01067 Connecting Screen

9. Once connected, the advertisement data and attribute fields can be viewed (see [Figure 30](#)).

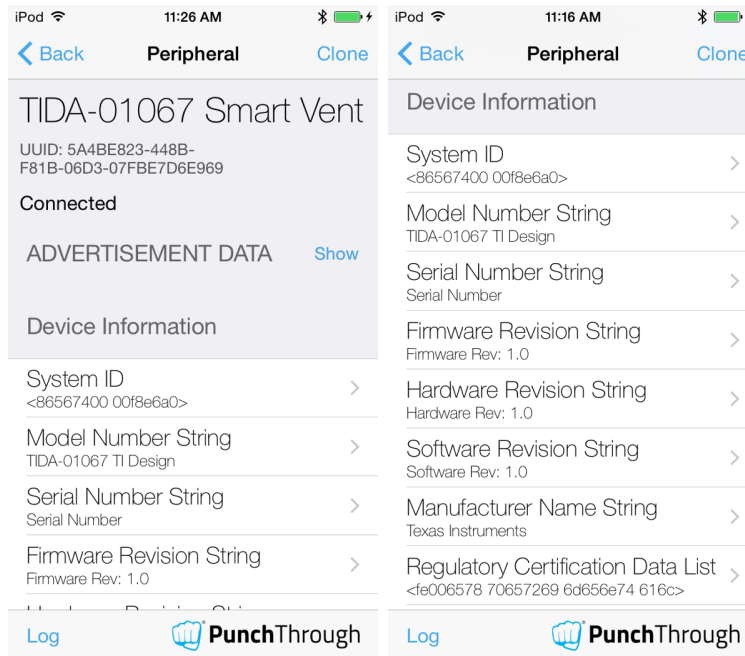


Figure 30. Advertisement Data Screen

10. Scroll to the bottom of the screen, and click on the *Vent Pos.* attribute (see [Figure 31](#)).



Figure 31. Attributes Screen

- After clicking the Vent Pos. attribute, the device automatically reads the current Vent Position state. At reset the vent will be turn to half way open (value: 0x03). In [Figure 32](#), the fully open position the value is 0. To change the value, click on the *Write new value* option. On the Android™ B-BLE app, the user must write two characters, meaning 00,01, 02, ... 06.

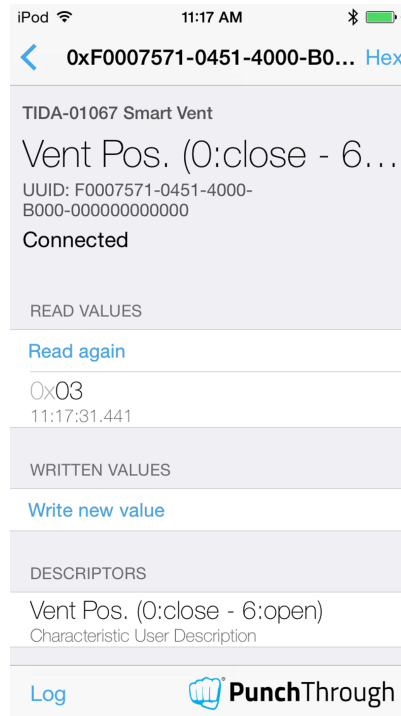


Figure 32. Vent Position Values Screen

- Write the value 1 in the text box, and click done (see [Figure 33](#)). This triggers the attribute value change event, which turns the motor.

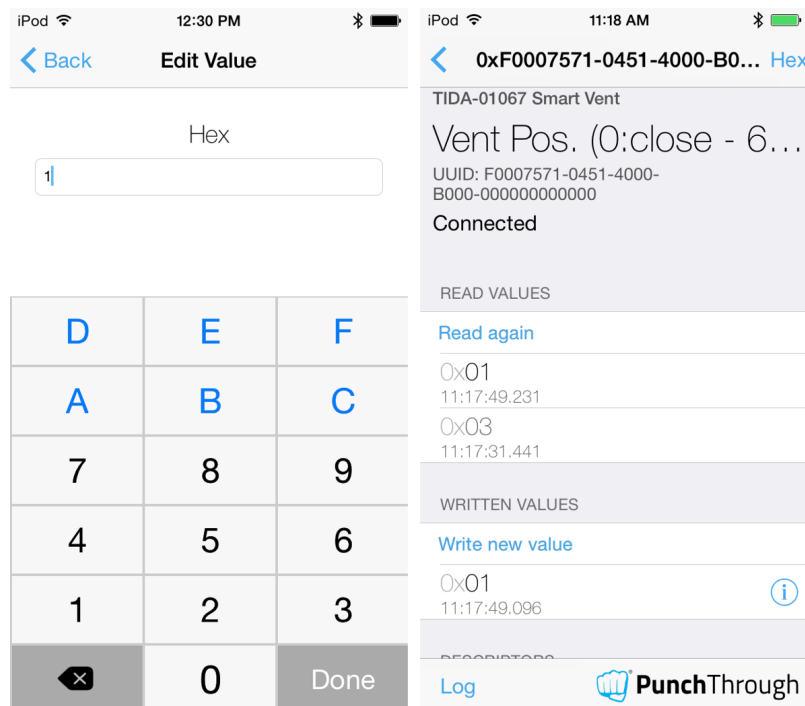


Figure 33. Selecting Vent Position State Value (1)

- Write a value 0 to 6 in the text box (see [Figure 34](#)), and click *Done* to adjust the vent louver to that position. If it is already in that position the motor will not move.

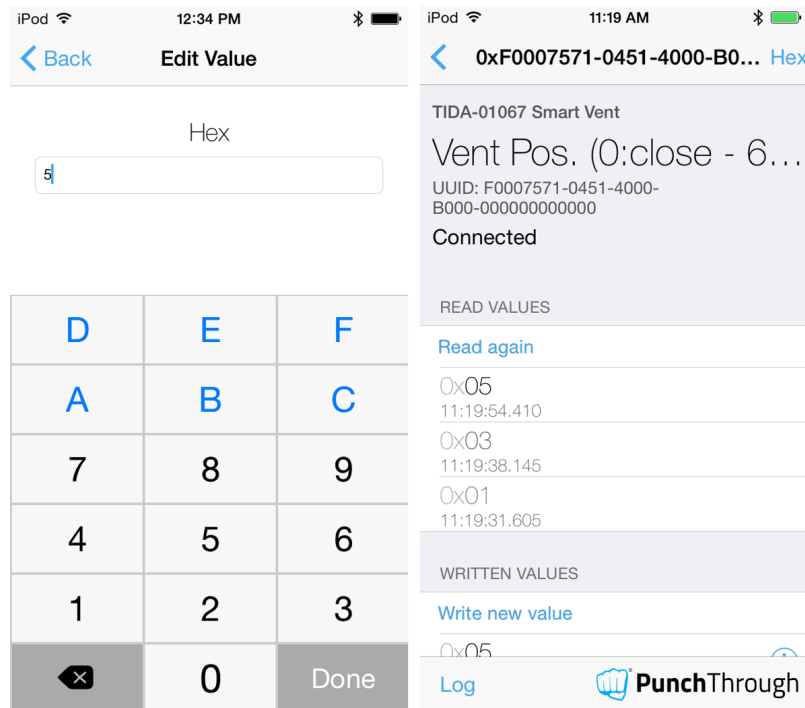


Figure 34. Selecting a Louver Position Value (5)

- If a new value is not written within 30 seconds, the inactivity time-out event is triggered and disconnects the device (see [Figure 35](#)).

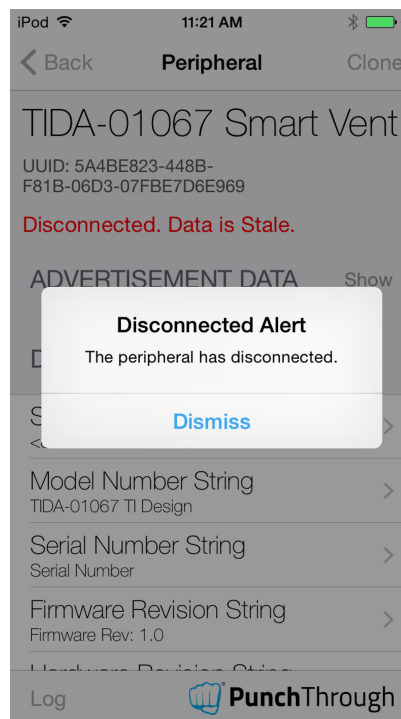


Figure 35. Inactivity Time-out Screen

4 Testing and Results

4.1 Test Setup

Each of the different subsystems within the TIDA-01067 reference design were tested independently when possible to achieve a breakdown of power statistics which are summarized in [Section 4.2.6](#). This section of the document outlines how the tests were set up and conducted, if a user wants to recreate the results.

4.1.1 Power Supply

To standardize the results, the reference design is powered by a 5-V power supply because the batteries normally used to power the design can decrease in voltage over time. The testing voltage is 5 V because the batteries balance out at 5 V for the majority of the life of the batteries. Keep in mind that batteries have a current draw limit, whereas the power supply does not. Measurements were taken with batteries as a comparison because of the innate current limit of the batteries and are discussed as well. The power supply was connected to J1 and the ground test point, as shown in [Figure 36](#). [Figure 36](#) also shows the configuration of the current probe used to capture the higher current motor drive waveforms.

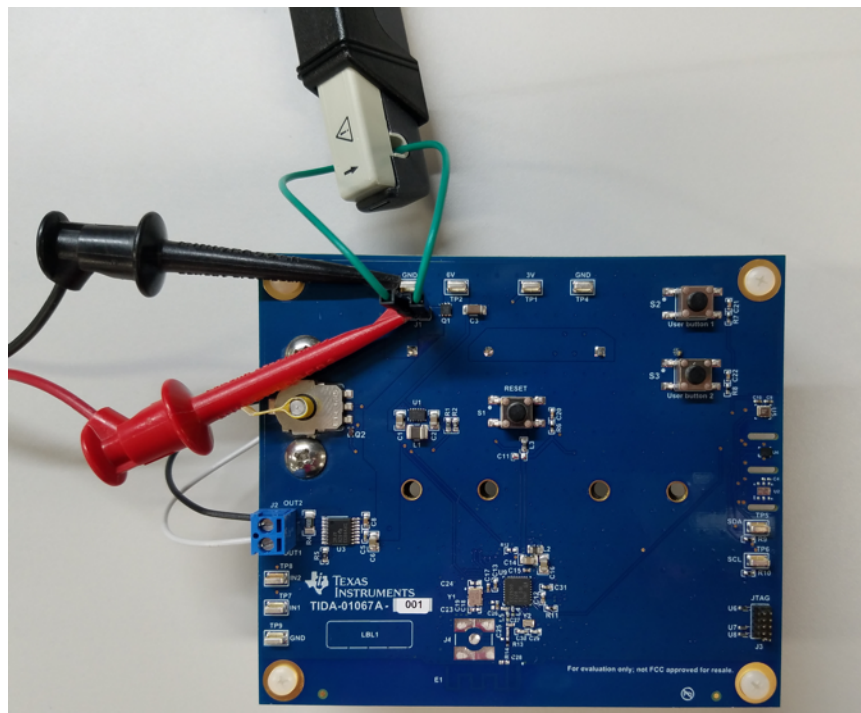


Figure 36. 5-V Power Supply Connection Configuration

4.1.2 Scope and Waveform Capture

A Tektronix® DPO 7054 Digital Phosphor Oscilloscope was used to capture the majority of the waveforms featured in this document. The Digital Phosphor Oscilloscope provides quick and easy capture of waveforms with averaging and peak values. The scope averages the points between horizontal markers to instantly give an accurate average, instead of just averaging the entire range on screen. The average calculated by the scope is implemented in the test results. A sense resistor was used when a current probe could not be used to measure the small amount of current for a specific test. The sense resistor is placed across the terminals of J1, as shown in [Figure 37](#). A multimeter was used to accurately measure the resistance of the sense resistor before putting the resistor into the circuit.

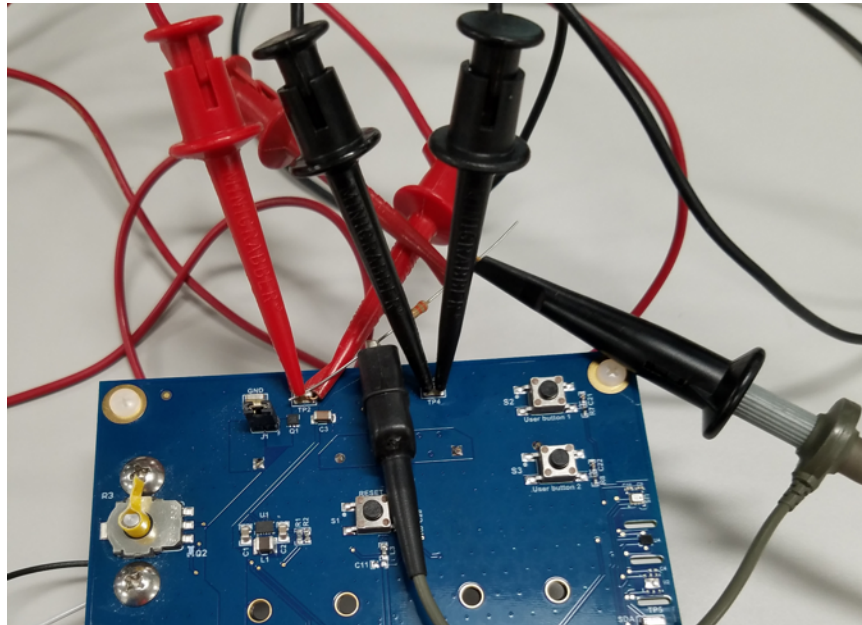


Figure 37. Sense Resistor Test Configuration on J1

4.1.3 Motor Loading

The rotary potentiometer on the board can make it difficult to connect the motor with an existing HVAC vent. A linkage could be designed with a worm gear and a few gears to manipulate a vent. The testing did not take into effect the extra load of a hard to move vent or a larger motor. However, a DC micro metal gear motor that is geared down to 15 RPM at 3 V and 0.3 A is installed into the TIDA-01067 design. The micro gear motor is similar to what is on some of the retrofit vents available on the market today. This motor should supply enough torque to drive other vents currently on the market.

4.2 Test Results

NOTE: Unless otherwise noted, the test data in the following sections was measured with the system at room temperature. All of the measurements in this section were measured with calibrated lab equipment.

4.2.1 Power System Tests

4.2.1.1 Buck Output and Efficiency

The input voltage at J1 varied from 6.4 V to 3.7 V, and the voltage on the 3-V rail was measured at TP1 and TP2. [Table 3](#) lists the results.

Table 3. Input Voltage Versus Buck Output

INPUT VOLTAGE (V)	BUCK OUTPUT (V)
6.4	3.0
6.0	3.0
5.6	3.0
5.2	3.0
5.0 (nominal)	3.0
4.8	3.0
4.4	3.0
4.0	3.0
3.7	3.0

The efficiency of the TPS62745 was simulated with TI's WEBENCH® Design Tool. The graphs in [Figure 38](#) and [Figure 39](#) show the results.

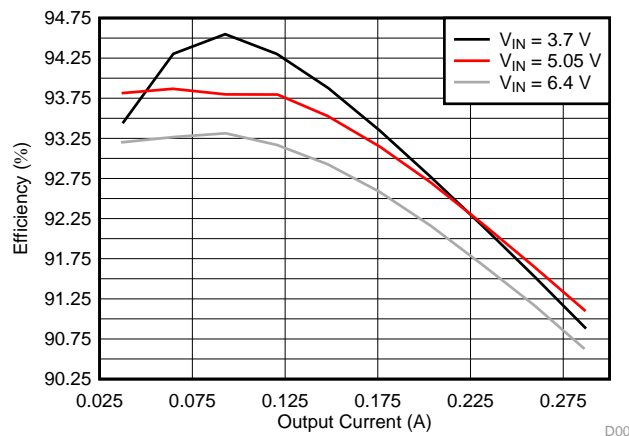


Figure 38. Buck Output Current Versus Efficiency (TPS62745)

Figure 39 shows a wider current range of the efficiency results.

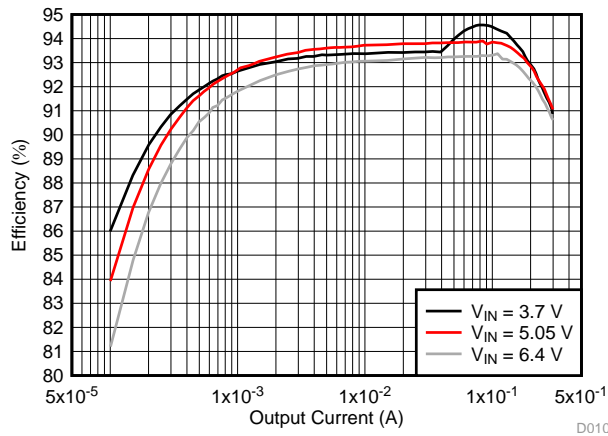


Figure 39. Buck Output Current Versus Efficiency, Wider Current Range (TPS62745)

4.2.1.2 Input Voltage Versus Average Current Consumption

The batteries decrease in voltage over time, but settle at a nominal voltage of 5 V. The majority of the testing done on the TIDA-01067 reference design is completed at the nominal voltage of 5 V with a power supply. However, batteries have innate current limiting, and the results may vary slightly depending on which batteries are used and how old they are, whereas the power supply has no current limit. Table 4 captures and records the peak current and average current for the motor operation state. The range of 6.4 V to 3.7 V was chosen because the maximum voltage of four AA batteries can be close to 6.4 V and the minimum V_{IN} of the buck is 3.7 V.

Table 4. Input Voltage Versus Average Current

INPUT VOLTAGE	PEAK CURRENT (mA)	AVG CURRENT (mA)	BUCK OUTPUT (V)
6.4	86.44	21.90	3.0
6.0	76.02	21.42	3.0
5.6	68.86	20.17	3.0
5.2	65.30	19.50	3.0
5.0 (nominal)	60.62	19.38	3.0
4.8	58.86	18.94	3.0
4.4	58.62	18.72	3.0
4.0	81.12	20.61	3.0
3.7	77.92	22.19	3.0

4.2.2 Bluetooth Low Energy Communications

The Bluetooth low energy tests included looking at the advertisement packet timing and current consumption waveforms, along with examining the connected packet timing and current waveforms. A sense resistor was used to measure the small amount of current in the system during the Bluetooth connection periods. Section 4.1 describes the sense resistor method.

Figure 40 shows the equivalent current waveform. The voltage readings were averaged over the time of the packet pulse time and a 50.048-Ω sense resistor was used.

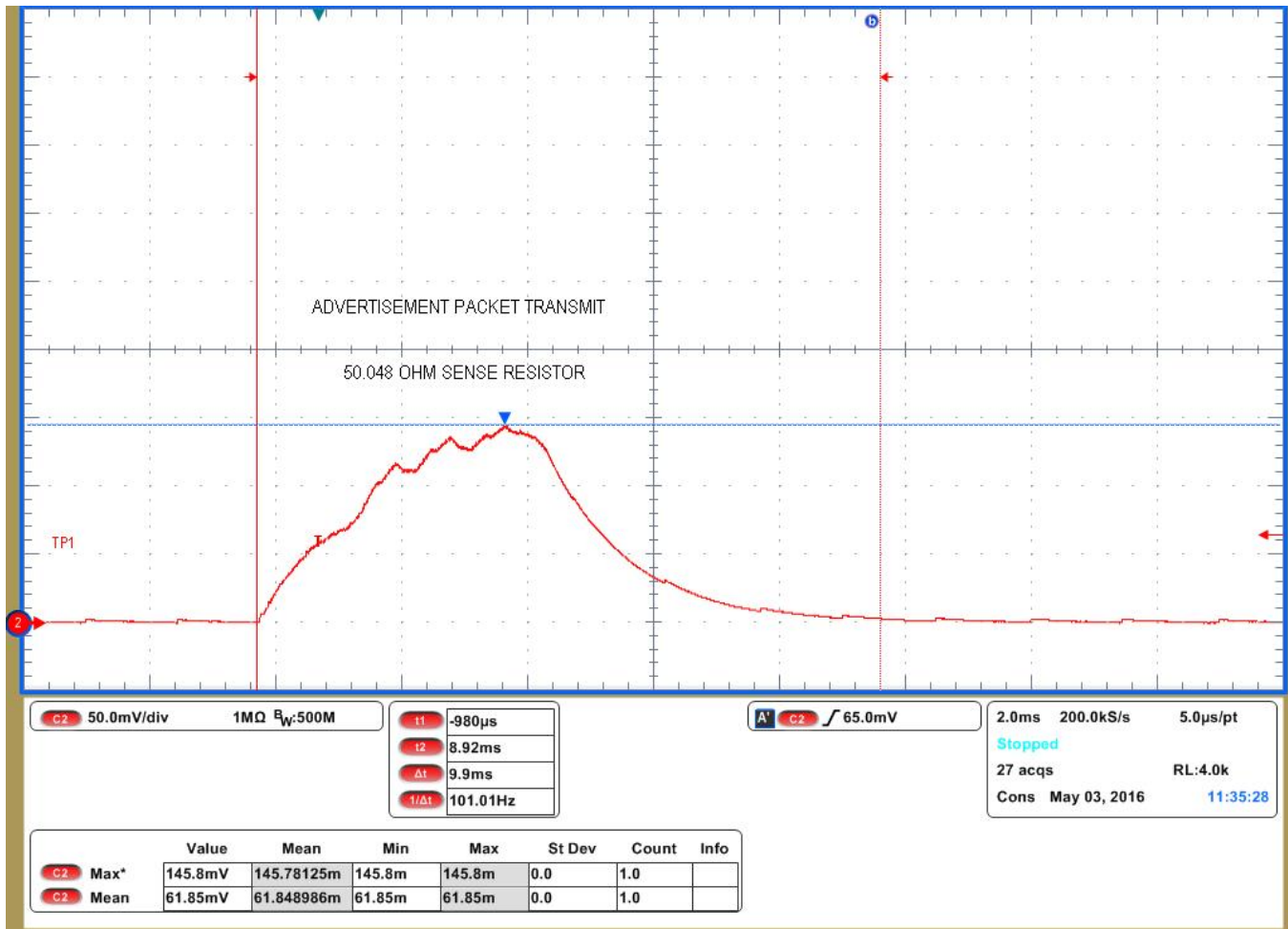


Figure 40. Bluetooth Low Energy Advertisement Packet

The average voltage is 61.849 mV, so dividing voltage by resistance allows us to solve for average current. The average current is 1.236 mA over the pulse width of approximately 9.9 ms.

$$\text{Average current} = (61.849 \text{ mV}) / (50.048 \Omega) = 1.236 \text{ mA}$$

(14)

Figure 41 shows the advertisement packet transmit period. The TIDA-01067 reference design broadcasts its basic information and advertises its presence to allow devices to connect to it every 500 ms. Figure 41 is the zoomed out view of the advertisement pulses seen in Figure 40. The tiny pulses seen between the transmits are the internal DC-DC converter of the CC2650 charging up for the next transmission.

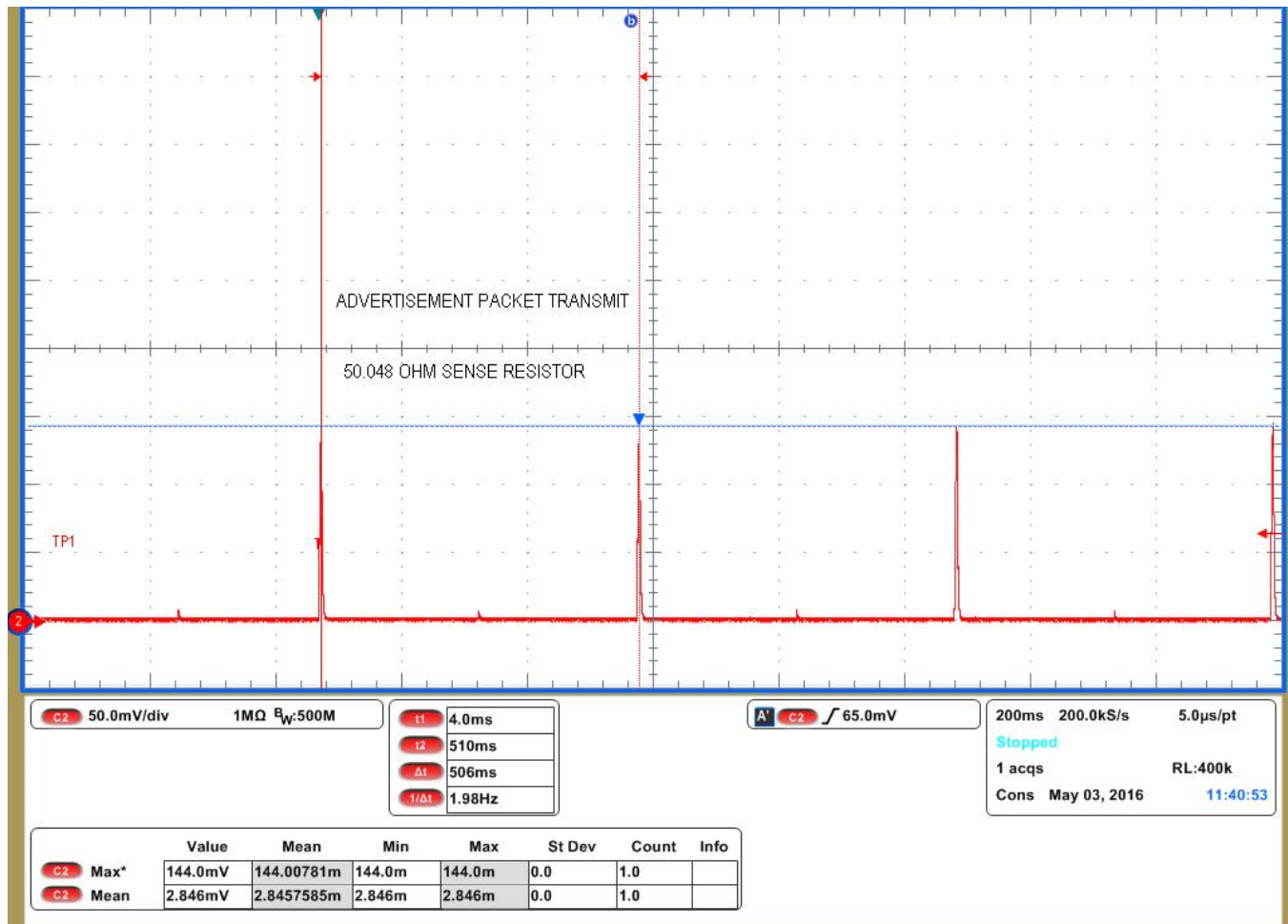


Figure 41. Bluetooth Low Energy Advertisement Transmit Period

Once a device is paired with the TIDA-01067 reference design the current consumption of the design looks slightly different. Figure 42 shows what the waveform of each connected pulse looks like. The maximum voltage is slightly lower and the pulse length is shorter.

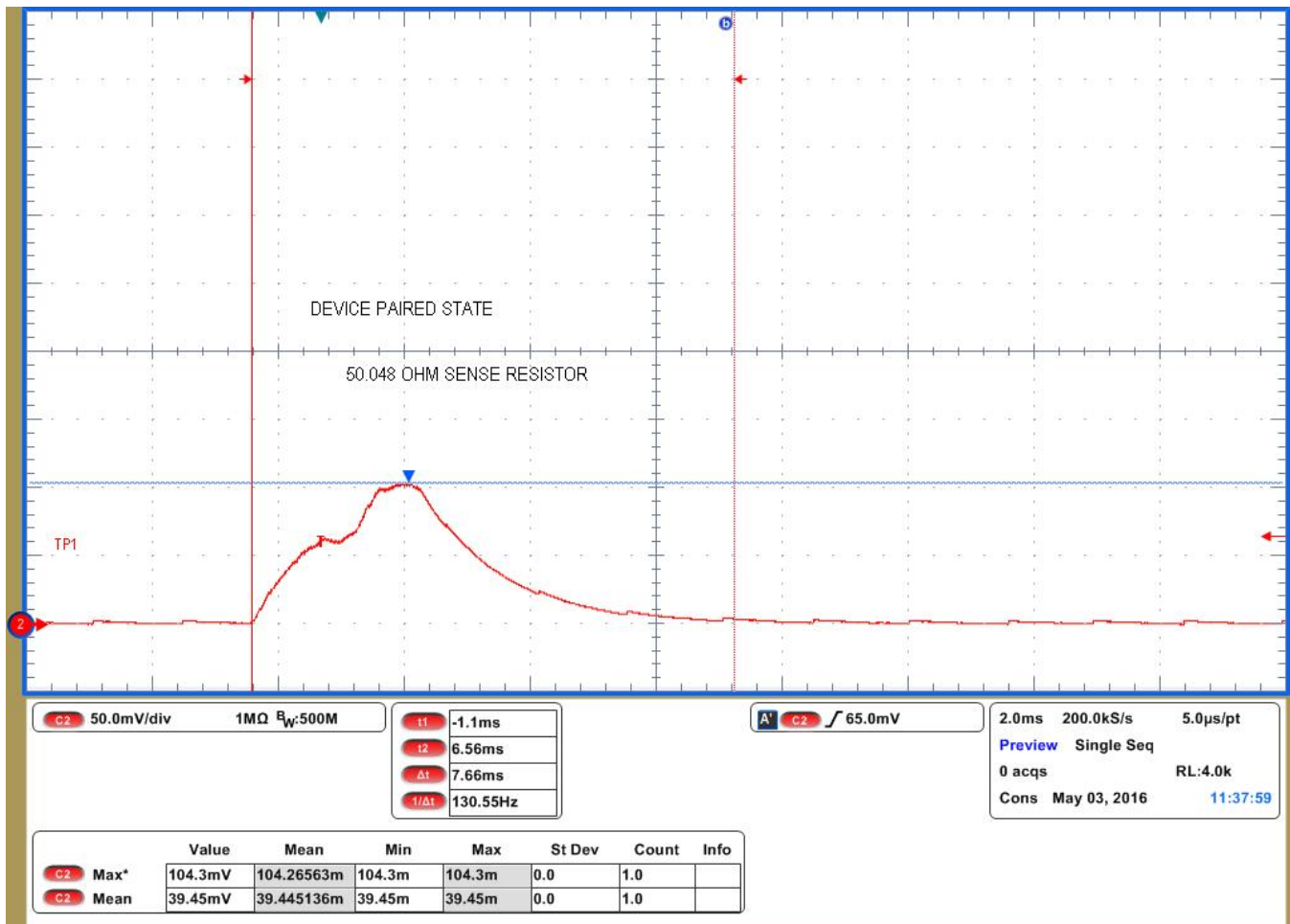


Figure 42. Bluetooth Low Energy Device Paired Packet

Equation 15 describes how to calculate the average current for the connected pulse.

$$\text{Average current} = (39.445 \text{ mV}) / (50.048 \ \Omega) = 0.788 \text{ mA} \tag{15}$$

The average current for a single connected pulse lasting approximately 7.66 ms = 0.788 mA.

Once a device is connected to the TIDA-01067 reference design, the average current pulse becomes slightly smaller. However, the pulse period is shortened to decrease latency in the user experience.

As seen in Figure 43, the period is 30 ms when a device is connected. The 30-ms transmit period stays in effect for 30 seconds after the last input from the user's device. More discussion of the software algorithm is discussed in Section 2.3.14.

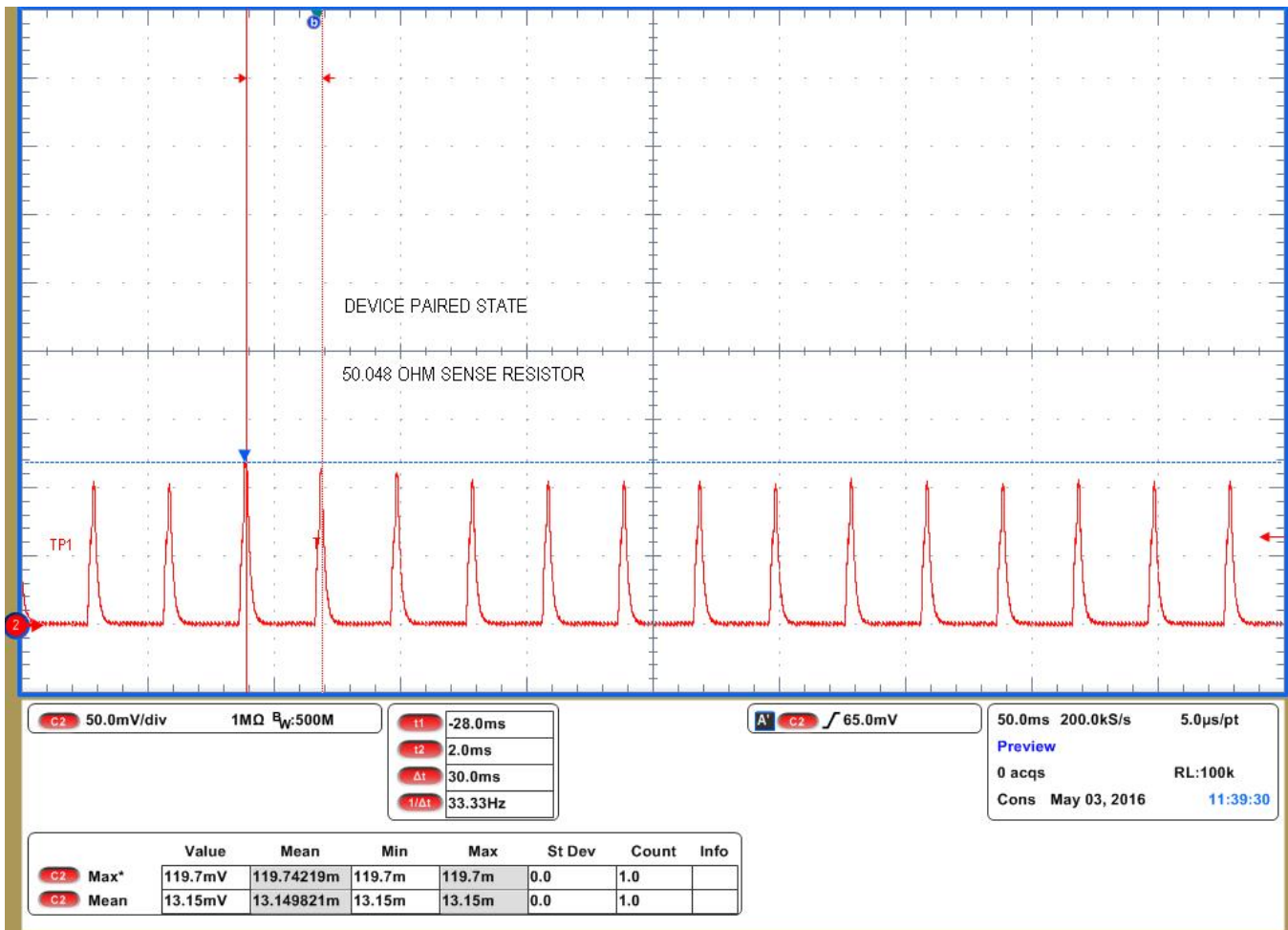


Figure 43. Bluetooth Low Energy Device Paired Packet Transmit Period

4.2.3 Standby Current

The average standby current can be found by measuring the current consumption between advertisement packet transmissions. During this time the other devices in the TIDA-01067 reference design are in standby or sleep mode, allowing an accurate measurement of the standby current. A small sense resistor was used to measure the small amount of current. The average standby current of this reference design with the algorithm discussed in Section 2.3.14 is approximately 3.7 μ A.

4.2.4 Motor Current

This section covers each of the different motor current waveforms for a louver adjustment event and a louver adjustment while bluetooth connected. The motor was free spinning while connected to the board through the rotary potentiometer sensor. A non-connected event may happen since a custom software algorithm could adjust the position depending on the environmental data. For each adjustment event the worst case was considered. The worst case being moving from the completely open position to closed or vice versa, on this reference design that is 180 degrees of motor spin. A 3.311-Ω sense resistor was used in this part of motor testing because of the low-current waveforms.

4.2.4.1 Motor Current Waveforms

Batteries have innate current limiting and because of this feature the maximum current spike when the motor started spinning may be different, average current of ≈ 21.10 mA over the 1.8-second louver adjustment event. Figure 44 shows the fully open to close event, and the reference design is being powered by the 5-V power supply. The starting current spike is larger because the power supply is not limiting the current. The current spike is ≈ 77 mA.

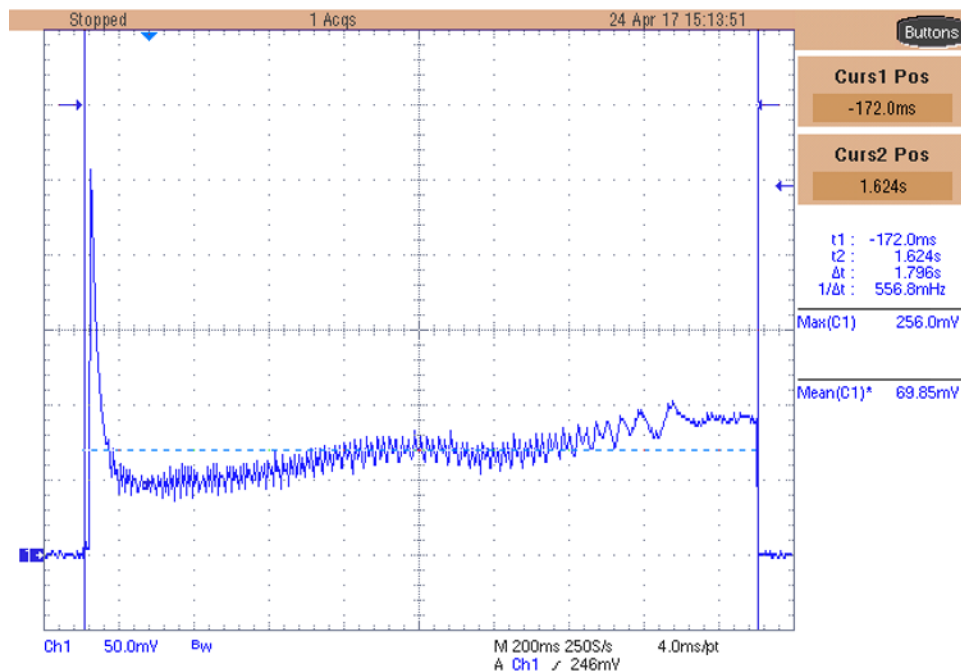


Figure 44. Louver 100% Open to 100% Closed (Bluetooth Low Energy Connected)

From now on, only the waveforms captured while the reference design is powered by the power supply are used to calculate the current consumption to standardize the results. The testing voltage is 5 V because the batteries balance out at 5 V for the majority of the life of the batteries. One thing to remember is that batteries have a current draw limit, whereas the power supply does not. Therefore, for higher current motors, the current spike may be different depending on the power source.

Figure 45 shows the voltage waveform with a 3.311-Ω sense resistor of the vent close event as initiated by the push-button without the Bluetooth connected. A current spike of 74.30 mA starts the motor with an average current of 19.33 mA.

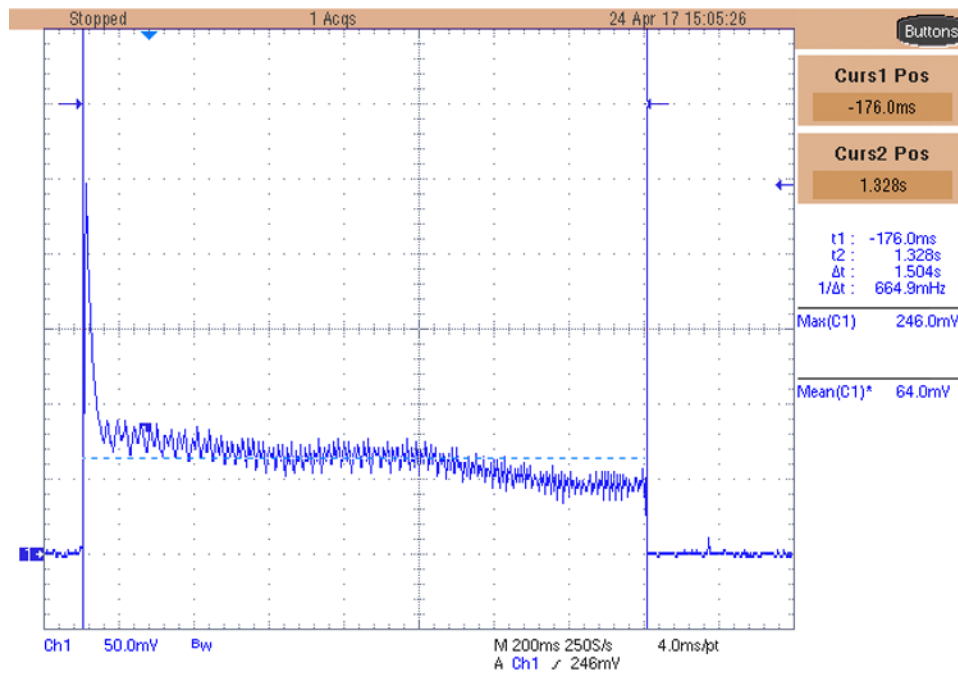


Figure 45. Louver 100% Open to 100% Closed (Bluetooth Low Energy Disconnected)

4.2.4.2 Motor Current Summary

Table 5 summarizes all the results of the motor testing. The 5-V power supply was used to standardize instead of using batteries, which give varying results because of battery drain.

Table 5. Motor Results Summary

MOTOR CONFIG (5 V)	PEAK CURRENT (mA)	AVERAGE CURRENT (mA)
180° adjustment (Bluetooth low energy connected)	77.32	21.10
180° adjustment (no Bluetooth low energy connected)	74.30	19.33

4.2.5 Environmental Sensing Current

Environmental sensing is another building block of this reference design and the smart damper end equipment. Using low-power sensors and periodically triggering the environmental sensors to take data can conserve battery life. Measuring the environment consists of triggering the HDC1010 and the BMP280 pressure sensor once an hour for preventative maintenance or HVAC diagnostics. Figure 46 shows the advertisement packets and the small spike is where the environmental sensing occurs. The cursors are highlighting this 120-ms time where the sensors are running. The average current over this time is 105.2 μ A. A 50.02- Ω sense resistor was used to capture this waveform. A shorter period can be implemented and there will be a negligible change in battery life because of the low average current and the limited time spent taking measurements.

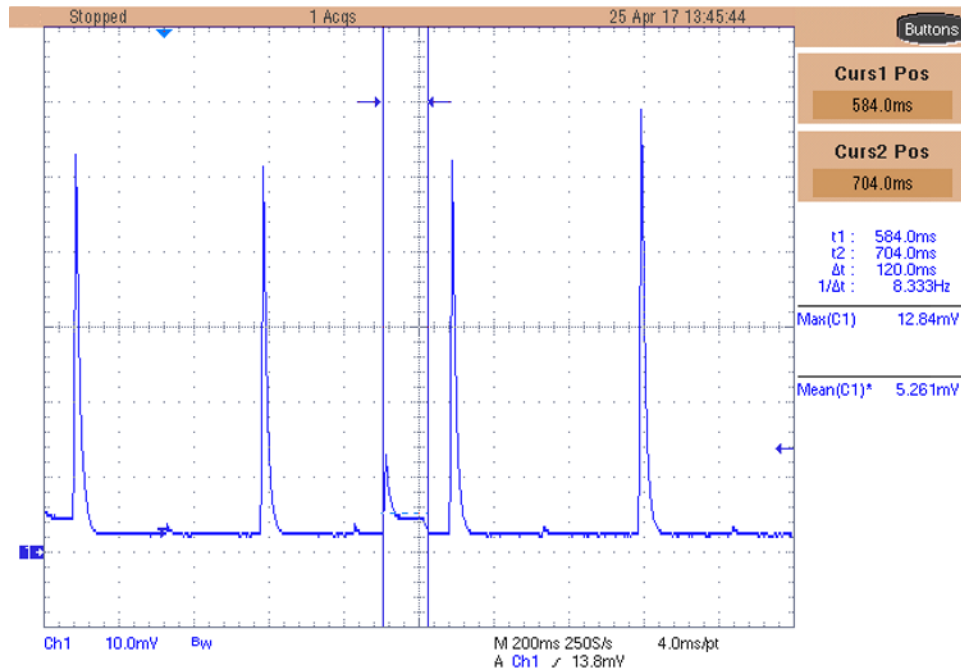


Figure 46. Environmental Sensing Waveform

4.2.6 Estimated Battery Life

To easily calculate the estimated battery life, each of the TIDA-01067 reference design states have been separated. The average current for standby, Bluetooth low energy advertisement, Bluetooth low energy connected, environmental sensing, and motor states have been gathered during testing. The average current per event, time per event, and total time in that state must be calculated or measured to estimate how much current is consumed in each state. A 24-hour time frame is used for the calculations because five louver adjustment events are being assumed in a 24-hour period. This 24-hour period also makes calculating battery life in years easier to convert.

NOTE: Unless otherwise noted, the battery capacity calculations in the following sections are done in mAh and not mWh.

4.2.6.1 Motor Average Current

The average current for the motor was measured in [Section 4.2.4](#). The highest current-consumption measurement is considered for these current calculations. An average current of 21.10 mA for 1.8 seconds was measured during the louver adjustment event. To find the average current consumption over a 24-hour period use [Equation 16](#) and [Equation 17](#).

$$\text{Duty Cycle of Motor State} = \text{Events} \times \text{Event Duration} \times \frac{1}{24 \text{ hours}} \times \frac{1}{60 \text{ mins}} \times \frac{1}{60 \text{ seconds}} \quad (16)$$

$$\text{Motor } I_{\text{avg}} = \text{LED and Motor } I_{\text{avg}} \times \text{Events} \times \text{event duration} \times \frac{1}{24 \text{ hrs}} \times \frac{1}{60 \text{ mins}} \times \frac{1}{60 \text{ secs}} \quad (17)$$

$$\text{Motor } I_{\text{avg}} = 21.10 \text{ mA} \times 5 \times 1.8 \text{ seconds} \times \frac{1}{24 \text{ hrs}} \times \frac{1}{60 \text{ mins}} \times \frac{1}{60 \text{ secs}} \quad (18)$$

$$\text{Motor } I_{\text{Avg}} = 2.198 \mu\text{A}$$

4.2.6.2 Bluetooth Low Energy Connected State Average Current

Because the average current for a single Bluetooth low energy connected pulse was measured, the total current consumption for 24-hour period can be calculated. The average current is 0.788 mA for 7.6 ms. The number of Bluetooth low energy connected pulses in the 30-second connected time must be calculated. The LED and motor current measurement included the connected pulses, so the motor event lasting 2 seconds must be subtracted from the connected period. The connection period is the time between pulses, or 30 ms.

$$\# \text{BLE Connected pulses per event} = \frac{\text{Connected Time} - \text{Motor Event Time}}{\text{Connection Period}} \quad (19)$$

$$\# \text{BLE Connected pulses per event} = \frac{30 \text{ sec} - 1.8 \text{ sec}}{0.03 \text{ sec}} \quad (20)$$

$$\text{Duty Cycle of Connected State} = \text{BLE Connected Pulses} \times \text{Events} \times \text{Event Duration} \times \frac{1}{24 \text{ hrs}} \times \frac{1}{60 \text{ mins}} \times \frac{1}{60 \text{ secs}} \quad (21)$$

$$\text{Connected } I_{\text{avg}} = \text{Connected } I_{\text{avg}} \times \text{BLE Connected Pulses} \times \text{Events} \times \text{Event Duration} \times \frac{1}{24 \text{ hrs}} \times \frac{1}{60 \text{ mins}} \times \frac{1}{60 \text{ secs}} \quad (22)$$

$$\text{Connected } I_{\text{avg}} = 0.788 \text{ mA} \times \frac{30 - 1.8}{0.03 \text{ sec}} \times 5 \times 0.0076 \text{ sec} \times \frac{1}{24 \text{ hrs}} \times \frac{1}{60 \text{ mins}} \times \frac{1}{60 \text{ secs}} \quad (23)$$

$$\text{Connected } I_{\text{avg}} = 0.326 \mu\text{A}$$

4.2.6.3 Bluetooth Low Energy Advertisement State Average Current

The average current during the Bluetooth low energy advertisement pulse is 1.235 mA over 9.9 ms. The CC2650 is sending advertisement packets only when it is not connected to a device, or when the motor is running; therefore, these periods must be subtracted from the run time of the Bluetooth low energy advertisement state.

$$\#BLE \text{ Advertisement packets} = \frac{24 \text{ hrs} \times 60 \text{ mins} \times 60 \text{ secs} - (\text{Connected Time} \times \text{Events})}{\text{Advertising Period}} \quad (24)$$

$$\text{Duty Cycle of Advertisement State} = \text{BLE Advertisement Pulses} \times \text{Pulse Duration} \times \frac{1}{24 \text{ hrs}} \times \frac{1}{60 \text{ mins}} \times \frac{1}{60 \text{ secs}} \quad (25)$$

$$\text{Advertisement } I_{\text{avg}} = \text{Advertisement } I_{\text{avg}} \times \text{BLE Advertisement Pulses} \times \text{Event} \times \text{Event Duration} \times \frac{1}{24 \text{ hrs}} \times \frac{1}{60 \text{ mins}} \times \frac{1}{60 \text{ secs}} \quad (26)$$

$$\text{Advertisement } I_{\text{avg}} = 1.235 \text{ mA} \times \frac{86400 - (30 \times 5)}{0.5 \text{ sec}} \times 0.0099 \text{ sec} \times \frac{1}{24 \text{ hrs}} \times \frac{1}{60 \text{ mins}} \times \frac{1}{60 \text{ secs}} \quad (27)$$

$$\text{Advertisement } I_{\text{avg}} = 24.41 \mu\text{A}$$

4.2.6.4 Average Environmental Sensing Current

Environmental sensing occurs once every hour and takes approximately 120 ms with an average current of 0.1052 mA. The following equations calculate the average current consumption over a 24 hour period.

$$\text{Duty Cycle of Environmental Sensing} = \text{Event} \times \text{Event Duration} \times \frac{1}{24 \text{ hrs}} \times \frac{1}{60 \text{ mins}} \times \frac{1}{60 \text{ secs}} \quad (28)$$

$$\text{Sensing } I_{\text{avg}} = \text{Sensing } I_{\text{avg}} \times \text{Events} \times \text{event duration} \times \frac{1}{24 \text{ hrs}} \times \frac{1}{60 \text{ mins}} \times \frac{1}{60 \text{ secs}} \quad (29)$$

$$\text{Sensing } I_{\text{avg}} = 0.1052 \text{ mA} \times 24 \times 0.12 \text{ seconds} \times \frac{1}{24 \text{ hrs}} \times \frac{1}{60 \text{ mins}} \times \frac{1}{60 \text{ secs}} \quad (30)$$

$$\text{Sensing } I_{\text{avg}} = 0.0035 \mu\text{A}$$

4.2.6.5 Average Standby Current

The standby current was measured as the average current consumption between each Bluetooth low energy advertisement pulse. Therefore, to solve the amount of time the smart damper is in standby mode, subtract the amount of times the device is in other states from the total time (see Equation 31). Then, multiply the standby current by the percentage of total time it is in standby mode (see Equation 33). The measured standby current is 4.7 μA .

$$\text{Standby Time} = 24 \text{ hrs} \times 60 \text{ mins} \times 60 \text{ secs} - \#BLE \text{ Advertisement Pulses} \times \text{Pulse Duration} - \#BLE \text{ Connected Pulses} \times \text{Events} \times \text{Connected Pulse Duration} \quad (31)$$

The connected time includes the time that the damper is in the motor state.

$$\text{Time in Standby} = 86400 \text{ secs} - \frac{86400 - (\text{Connected Time} \times \text{Events})}{\text{Advertising Period}} \times \text{Pulse Duration} - \frac{\text{Connected Time} - \text{Motor Event Time}}{\text{Connection Period}} \times \text{Connected Pulse Duration} \times \text{Events} \quad (32)$$

$$\text{Standby } I_{\text{avg}} = 0.0037 \text{ mA} \times \left(86400 \text{ secs} - \frac{86400 \text{ secs} - (30 \text{ secs} \times \text{Events})}{0.5 \text{ secs}} \times 0.0099 \text{ secs} - \frac{30 \text{ secs} - 2 \text{ secs}}{0.03 \text{ secs}} \times 0.0076 \times \text{Events} \times \frac{1}{24 \text{ hrs}} \times \frac{1}{60 \text{ mins}} \times \frac{1}{60 \text{ secs}} \right) \quad (33)$$

$$\text{Standby } I_{\text{avg}} = 3.626 \mu\text{A}$$

4.2.6.6 Estimated Battery Life

The total system average current must be found to accurately estimate battery life. The total average current is found by adding each of the average currents (see [Table 6](#) and [Equation 34](#)).

Table 6. Current Consumption per State

STATE	AVERAGE CURRENT (μA)
Motor and LEDs	2.1980
Bluetooth low energy connected	0.3260
Bluetooth low energy advertisement	24.4100
Environmental sensing	0.0035
Standby	3.6260
Total average current	30.5600

$$\text{Battery Life in Years} = \frac{\text{battery Capacity (mAh)}}{\text{Avg Current (mA)}} \times \frac{1}{8760 \text{ hr / yr}} \times \text{derating factor} \quad (34)$$

The derating factor in [Equation 34](#) accounts for self-aging of the battery.

$$\text{Battery Life in Years} = \frac{3000 \text{ mAH}}{0.03056 \text{ mA}} \times \frac{1}{8760 \text{ hr / yr}} \times 0.90 \quad (35)$$

$$\text{Battery Life in Years} = 10.08$$

5 Design Files

5.1 Schematics

To download the schematics, see the design files at [TIDA-01067](#).

5.2 Bill of Materials

To download the bill of materials, see the design files at [TIDA-01067](#).

5.3 PCB Layout Recommendations

To ensure high performance, the TIDA-01067 reference design was laid out using a four-layer PCB. The second layer is a solid GND pour, and the third layer is used for power rail routing without a ground fill. The top and bottom layers are used for general signal routing and also have GND fills in unused areas. All of the TI products used in this TI Design adhere to the layout guidelines detailed in their respective datasheets. The onboard Bluetooth antenna was placed as far away from other noise sources as possible, such as the buck converter or other items that could act as an antenna (for example, test points or large traces).

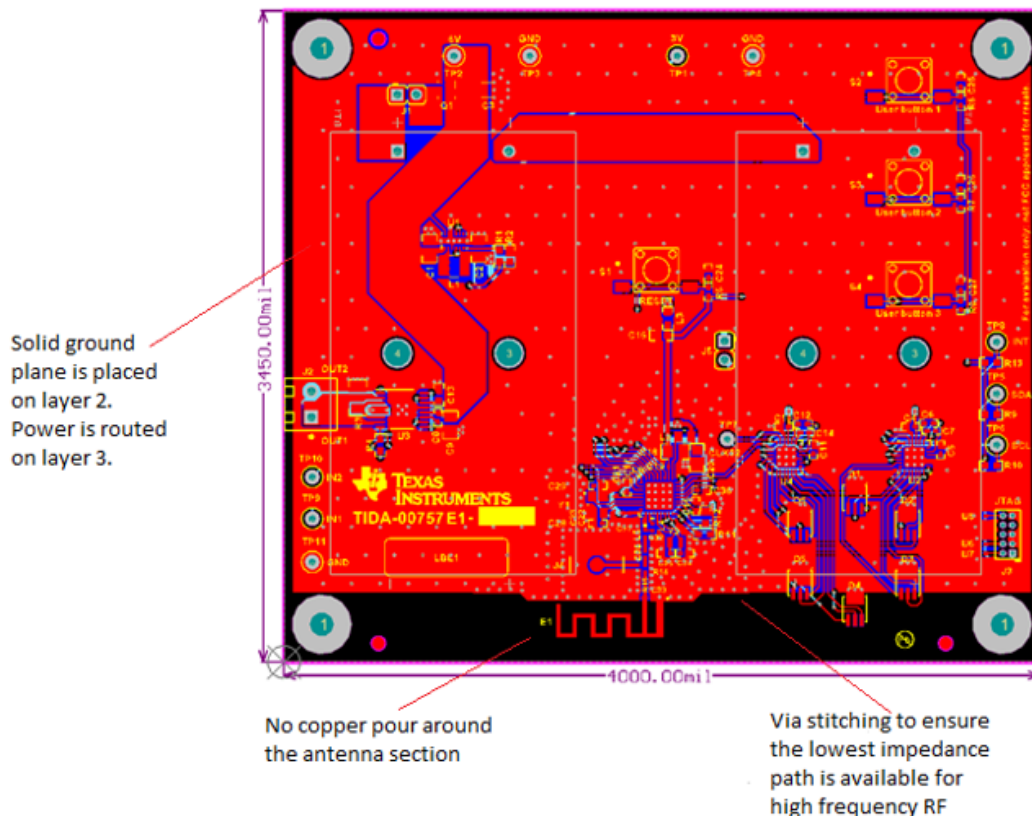


Figure 47. Smart Damper Reference Design Layout Guidelines

5.3.1 Layout Prints

To download the layer plots, see the design files at [TIDA-01067](#).

5.4 Altium Project

To download the Altium project files, see the design files at [TIDA-01067](#).

5.5 Gerber Files

To download the Gerber files, see the design files at [TIDA-01067](#).

5.6 Assembly Drawings

To download the assembly drawings, see the design files at [TIDA-01067](#).

6 Software Files

To download the software files, see the design files at [TIDA-01067](#).

7 Related Documentation

1. Texas Instruments, [Reverse Current Battery Protection Circuits](#), Application Report (SLVA139)
2. Texas Instruments, [Calculating Motor Driver Power Dissipation](#), Application Report (SLVA504)
3. Texas Instruments, [WEBENCH Design Center](#), (<http://www.ti.com/webench>)

7.1 Trademarks

SimpleLink, SmartRF, Code Composer Studio, DCS-Control, MSP430 are trademarks of Texas Instruments.

WEBENCH is a registered trademark of Texas Instruments.

Cortex is a registered trademark of ARM.

iPhone is a registered trademark of Apple Inc.

HomeKit, LightBlue are trademarks of Apple, Inc.

Apple is a registered trademark of Apple, Inc.

ARM is a registered trademark of Arm Limited.

Bluetooth is a registered trademark of Bluetooth SIG, Inc.

CoreMark is a registered trademark of Core-Mark International, Inc.

Energizer is a registered trademark of Energizer Holdings, Inc.

Android is a trademark of Google, Inc.

IAR Embedded Workbench is a registered trademark of IAR Systems AB.

Samsung, Galaxy S7 are registered trademarks of Samsung Electronics Co., Ltd.

Tektronix is a registered trademark of Tektronix, Inc.

ZigBee is a registered trademark of ZigBee Alliance.

8 About the Authors

JARROD KREBS is a systems designer at Texas Instruments, where he is responsible for developing reference designs in the industrial segment. Jarrod has experience with software and embedded applications implemented on ARM-based microcontrollers and TI's MSP430™ platforms. Jarrod earned his bachelor of science in computer engineering from Kansas State University in Manhattan, KS. Jarrod is also a member of the Institute of Electrical and Electronics Engineers (IEEE).

CHRISTINA S. LAM is a systems architect at Texas Instruments where she is responsible for developing firmware for reference design solutions in the industrial segment. Christina has broad experience with applications processors, microcontrollers, and digital-signal processors with specialties in embedded firmware. Christina earned her bachelor of science in electrical and computer engineering from the University of Texas at Austin.

IMPORTANT NOTICE FOR TI DESIGN INFORMATION AND RESOURCES

Texas Instruments Incorporated ("TI") technical, application or other design advice, services or information, including, but not limited to, reference designs and materials relating to evaluation modules, (collectively, "TI Resources") are intended to assist designers who are developing applications that incorporate TI products; by downloading, accessing or using any particular TI Resource in any way, you (individually or, if you are acting on behalf of a company, your company) agree to use it solely for this purpose and subject to the terms of this Notice.

TI's provision of TI Resources does not expand or otherwise alter TI's applicable published warranties or warranty disclaimers for TI products, and no additional obligations or liabilities arise from TI providing such TI Resources. TI reserves the right to make corrections, enhancements, improvements and other changes to its TI Resources.

You understand and agree that you remain responsible for using your independent analysis, evaluation and judgment in designing your applications and that you have full and exclusive responsibility to assure the safety of your applications and compliance of your applications (and of all TI products used in or for your applications) with all applicable regulations, laws and other applicable requirements. You represent that, with respect to your applications, you have all the necessary expertise to create and implement safeguards that (1) anticipate dangerous consequences of failures, (2) monitor failures and their consequences, and (3) lessen the likelihood of failures that might cause harm and take appropriate actions. You agree that prior to using or distributing any applications that include TI products, you will thoroughly test such applications and the functionality of such TI products as used in such applications. TI has not conducted any testing other than that specifically described in the published documentation for a particular TI Resource.

You are authorized to use, copy and modify any individual TI Resource only in connection with the development of applications that include the TI product(s) identified in such TI Resource. NO OTHER LICENSE, EXPRESS OR IMPLIED, BY ESTOPPEL OR OTHERWISE TO ANY OTHER TI INTELLECTUAL PROPERTY RIGHT, AND NO LICENSE TO ANY TECHNOLOGY OR INTELLECTUAL PROPERTY RIGHT OF TI OR ANY THIRD PARTY IS GRANTED HEREIN, including but not limited to any patent right, copyright, mask work right, or other intellectual property right relating to any combination, machine, or process in which TI products or services are used. Information regarding or referencing third-party products or services does not constitute a license to use such products or services, or a warranty or endorsement thereof. Use of TI Resources may require a license from a third party under the patents or other intellectual property of the third party, or a license from TI under the patents or other intellectual property of TI.

TI RESOURCES ARE PROVIDED "AS IS" AND WITH ALL FAULTS. TI DISCLAIMS ALL OTHER WARRANTIES OR REPRESENTATIONS, EXPRESS OR IMPLIED, REGARDING TI RESOURCES OR USE THEREOF, INCLUDING BUT NOT LIMITED TO ACCURACY OR COMPLETENESS, TITLE, ANY EPIDEMIC FAILURE WARRANTY AND ANY IMPLIED WARRANTIES OF MERCHANTABILITY, FITNESS FOR A PARTICULAR PURPOSE, AND NON-INFRINGEMENT OF ANY THIRD PARTY INTELLECTUAL PROPERTY RIGHTS.

TI SHALL NOT BE LIABLE FOR AND SHALL NOT DEFEND OR INDEMNIFY YOU AGAINST ANY CLAIM, INCLUDING BUT NOT LIMITED TO ANY INFRINGEMENT CLAIM THAT RELATES TO OR IS BASED ON ANY COMBINATION OF PRODUCTS EVEN IF DESCRIBED IN TI RESOURCES OR OTHERWISE. IN NO EVENT SHALL TI BE LIABLE FOR ANY ACTUAL, DIRECT, SPECIAL, COLLATERAL, INDIRECT, PUNITIVE, INCIDENTAL, CONSEQUENTIAL OR EXEMPLARY DAMAGES IN CONNECTION WITH OR ARISING OUT OF TI RESOURCES OR USE THEREOF, AND REGARDLESS OF WHETHER TI HAS BEEN ADVISED OF THE POSSIBILITY OF SUCH DAMAGES.

You agree to fully indemnify TI and its representatives against any damages, costs, losses, and/or liabilities arising out of your non-compliance with the terms and provisions of this Notice.

This Notice applies to TI Resources. Additional terms apply to the use and purchase of certain types of materials, TI products and services. These include; without limitation, TI's standard terms for semiconductor products (<http://www.ti.com/sc/docs/stdterms.htm>), [evaluation modules](#), and [samples](http://www.ti.com/sc/docs/sampterm.htm) (<http://www.ti.com/sc/docs/sampterm.htm>).

Mailing Address: Texas Instruments, Post Office Box 655303, Dallas, Texas 75265
Copyright © 2017, Texas Instruments Incorporated